REAL TIME VOLTAGE STABILITY MONITORING AND CONTROL USING SYNCHROPHASORS

By

XING LIU

A dissertation submitted in partial fulfillment of
the requirements for the degree of

DOCTOR OF PHILOSOPHY

WASHINGTON STATE UNIVERSITY
School of Electrical Engineering and Computer Science

August 2012

To the Faculty of Washington State University:

The members of the Committee appointed to examine the dissertation of Xing Liu find it satisfactory and recommend it be accepted.

_____

Vaithianathan Venkatasubramanian, Ph.D., Chair

_____

Anjan Bose, Ph.D.

_____

Luis G. Perez, Ph.D.

ACKNOWLEDGEMENT

I must show my strong appreciation to my major advisor and chairman, Professor Vaithianathan Venkatasubramanian because of his skilled guidance, warm dedication, valuable instruction and continuous support throughout my doctoral study at Washington State University in Pullman. The whole experience during these years will always be my treasure for my further research and even my further life as well. I have also enjoyed the enlightening instruction and advisement from Professor Anjan Bose and Professor Luis G. Perez and am grateful to their participation on my advisory committee.

Support from Power System Engineering Research Center (PSERC) is gratefully acknowledged. That research is mainly funded by Korean Electric Power Research Institute (KEPRI) on power system automatic voltage control. Another appreciation will be committed to Ritchie Carroll and Tennessee Valley Authority (TVA) for real Synchrophasors collection and testing implementation on power system voltage security real-time monitoring. I have to thank my advisor's former Ph.D. students, Yonghong Chen and Jingdong Su whose brilliant work gave me the solid start.

I will be missing my friends who have given me the friendships and the impressive time that accompanied my study and life in Washington State University.

I am always deeply indebted to my parents. Without their enduring love, I would never walk so far.

REAL TIME VOLTAGE STABILITY MONITORING AND CONTROL USING SYNCHROPHASORS

Abstract

by Xing Liu, Ph.D.
Washington State University
August 2012

Chair: Vaithianathan Venkatasubramanian

One new real-time Voltage Stability Monitoring framework and its corresponding Advanced Voltage Control scheme provide the possibility of improvement in voltage stability, security and control in power systems. They take full advantage of the new measurement method Synchrophasors in current bulk power system so that more accurate assessment and control action can be achieved in less time using complex information.

First, one real-time Voltage Stability Monitoring framework is developed to utilize the proposed "global voltage stability assessment index" to detect the weak buses. This framework could be a totally model-free design. For each individual bus, only the

information from the local PMUs is needed. So the proposed global voltage stability assessment index becomes possible by real time relation of the “Line Sensitivity”. That is, the line sensitivities are directly calculated from Synchrophasor measurements. Although this methodology is quite different from the classical ones which are widely used in current power systems, the conclusions from them are confident.

The Advanced Voltage Control scheme is the next step after assessment of voltage stability. This proposed control design is problem-oriented. All available SVCs, capacitor banks, reactor banks and LTC transformers will be included as potential control devices. The controller will select certain control devices to mitigate the system voltage violation so that the control actions will also satisfy other realistic requirements rather than the voltage limit constraints, such as the minimum switching cost and proper device priority. The controller will evaluate the control action by the line sensitivities attained by installed Synchrophasors at this bus and the other local buses.

Contents

List of Tables

List of Figures

Dedicated to My Parents

Chapter 1

Introduction

An electric power system is a network of electrical components used to supply, transmit and use electric power. An example of an electric power system is the network that supplies a region's homes and industries with synchronized effective power – for sizable regions, this power system is known as the grid and can be broadly divided into the generators that supply the power, the transmission system that carries the power from the generating centers to the load centers and the distribution system that feeds the power to nearby homes and industries. From the year of 1881 when the world's first power system was built in England to now, the power systems have experienced vast changes which took place everywhere, many theoretical or technical evolution led to the improvements which make the power system more stable and more reliable. However, new researches need to guarantee the power systems to be able to satisfy continuous the growing requirements. The fact is that the current power systems have become the most intelligent networks around world, which are composed of a large number of nodes and all kinds of equipments which can affect each others. By all means, to measure and control this network under

certain conditions is challenging. Apparently, two topics rise which are also very important aspects for the power systems: how to assess current systems and how to control them. In fact, this dissertation mainly focuses on these two aspects and plans to describe how the new technology, Synchrophasors which have been applied into the power systems recently, affects the current power system so that we can have not only more efficient and rapid ways to assess the current power systems but also more reliable and faster responses to control the systems. More specially, this dissertation will focus on the voltage stability related to the other areas in the power systems although the applications of Synchrophasors can be more comprehensive. Before we introduce the detailed content in this dissertation, simply imagine a normal situation that one operator of the power systems will see the measurement from SCADA lacking of certain detailed information, and then this operator will know the detailed system status from State Estimation(SE) and Energy Management System(EMS) running. Typically, this procedure will take several minutes which depends on the size of this system. Further, if some voltage issue is found, more time will be spent whether this operator would like to take the suggestion from some off-line modal studies or not. Also, this operator could not ensure this action is optimal or coordinated if the other nodes will be considered. But, with the help of Synchrophasors, if the whole process takes

only around several tens of seconds and also the control can be an on-line decision, optimal and coordinated.

After briefly presenting some basic theory, background and review in chapter 1, this dissertation will discuss new development.

1.1 SCADA and Synchrophasors

SCADA is an acronym for Supervisory Control And Data Acquisition. It is not exclusive for the power systems but general for the industrial control system: computer systems that monitor and control industrial, infrastructure, or facility-based processes. In power systems, SCADA systems are used to perform tasks such as switching on generators, controlling generator output and switching in or out system elements for maintenance. Today, SCADA systems are much more sophisticated, however, it cannot come up with the angles directly as we know which are relative quantities because of its definition. Fig 1.1 is showing an example of SCADA architecture. In application level, the State Estimation has to be used to access each status of the measured equipments.

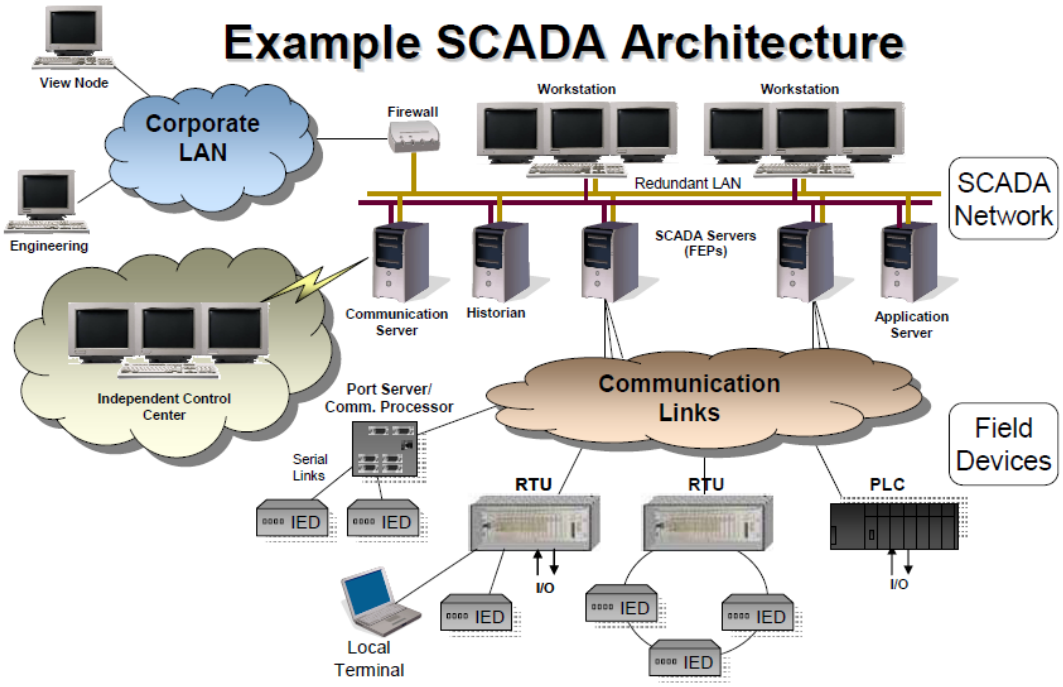

Figure 1.1 Example of SCADA Architecture [1]

Simply, as far as this point is concerned, Synchrophasors can provide a sufficiently accurate angle reference point from GPS satellite so that the angle information of the measured equipments can be accessed directly in the measurement level. The equipments in Synchrophasors measurement method are also called Phasor Measurement Units (PMUs). A demonstration of PMUs is shown in Fig 1.2.

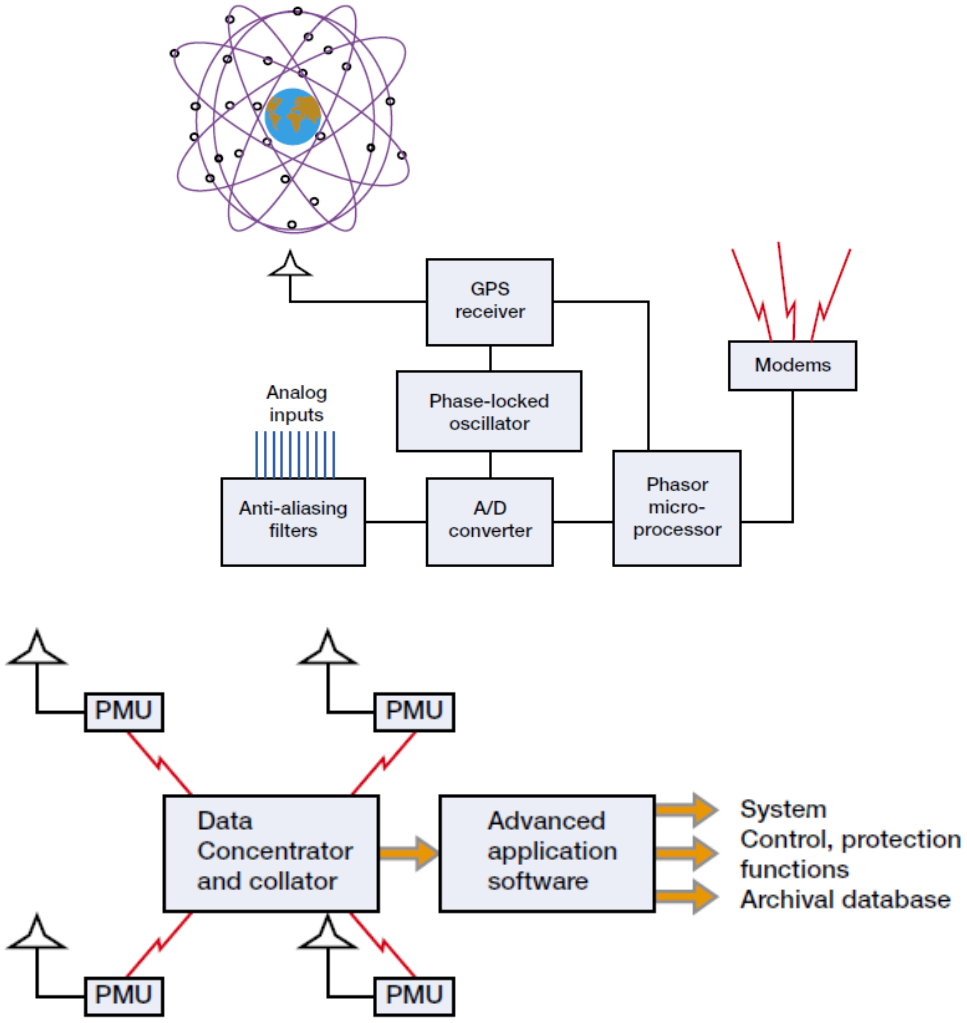

Figure 1.2 Example of PMUs Architecture [2]

With the application of a Global Positioning System (GPS), PMUs can provide a tool for system operators and planners to measure the state of electrical system and manage power quality. PMUs measure voltages and currents at diverse locations on a power grid and can output accurately time-stamped voltage and current phasors. Because these phasors are

truly synchronized, synchronized comparison of two quantities is possible in real time. These comparisons can be used to assess system conditions.

Since the Synchrophasors was invented by Dr. Arun G. Phadke and Dr. James S. Thorp in 1988[3], it has been used around the world in diverse applications: Voltage and current phasing verification, Substation voltage measurement refinement, SCADA verification and backup, Communication channel analysis, Wide-area frequency monitoring, Improved state estimation, Wide-area disturbance recording, Distributed generation control, Synchrophasor-assisted black start, Synchrophasor-based protection and so on. The detailed introduction of the basic theory of Synchrophasor would not be indicated because this dissertation focuses on one newly developed application of its. But, one important component must be illustrated first here in that the various applications can be realized. Certainly, the work of the voltage monitoring in this dissertation is based on this component as well. That component is called Phasor Data Concentrator (PDC). PDC is designed to collect the information tagged with an accurate time stamp from satellites and communication channels from Synchrophasors installed in the whole electric system. In fact, such a network is also known as Wide Area Measurement Systems (WAMS). The performance of PDC will influence on the results of those applications direction, on the contrary, the processed and time-aligned data from PDC will make the applications more

accurate, faster and powerful. Our work is based on one PDC platform: openPDC which is developed by the Grid Protection Alliance which was part of Tennessee Village Authority (TVA) before May, 2010. In terms of the official definition, *The openPDC is a complete Phasor Data Concentrator software system designed to process streaming time-series data in real-time. Measured data gathered with GPS-time from many hundreds of input sources is time-sorted and provided to user defined actions as well as to custom outputs for archival.* Fig 1.3 easily shows the functionalities of openPDC [4].

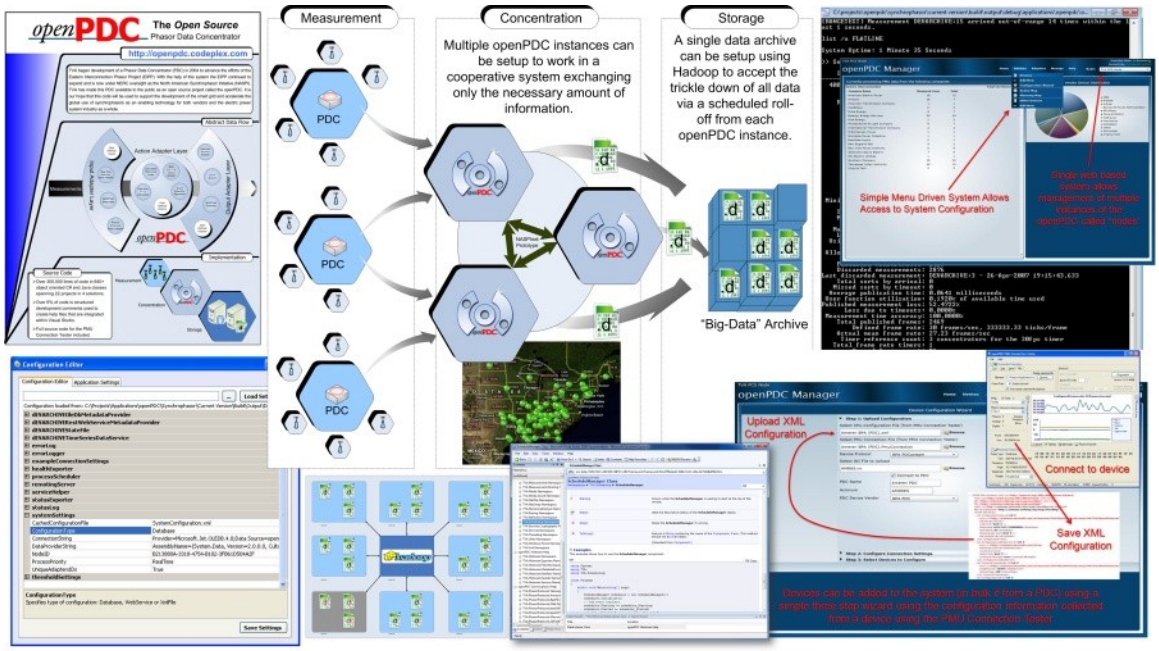

Figure 1.3 Framework of openPDC [4]

1.2 Motivation and Background

Voltage stability is always an operational reliability for modern power systems. With the growing demand in loads, the power transfers have been increasing steadily. The power systems can operate in many different operating conditions in that the power transfer has become more unpredictable because of many factors such as power market deregulation, unscheduled voltage regulation, transmission line outage and so on. All of them can push transmission systems to operate close to the limits which heavily influence the voltage stability. Consequently, the efficient and effective monitoring and control of the voltage are crucial for security and reliability of the power systems.

The main voltage monitoring and control are based on SCADA and EMS currently. Due to the limitations of this measurement, e.g., slow data sampling rate, slow data communication rates, time consuming computation in state estimation etc., it will take minutes to give the whole picture of measured electric system. Thus, operators hardly access the real time and detailed voltage and current vectors so that on-line voltage control will not be realistic. On the other hand, if we have the data which has high-sampling rate, high speed communication channels, full information of the measured points, how can we take advantage of these technological advance.

Currently, this advanced measurement method has been recognized widely and many measurement networks based on Synchrophasors have been installed around the world. In North America, the US Western Power System already has a network of phasor of PMUs with continuous recording to capture disturbance events. The Eastern Interconnected Power System has formally started a similar network under Smart Grid Investment Grants. In other words, plenty of wide-area synchrophasor systems are becoming available. To some extent, this attributes to several projects recently done by Washington State University (WSU), which were funded by Power System Engineering Research Center (PSERC), Tennessee Valley Authority (TVA), Entergy, Bonneville Power Administration (BPA) and US Department of Energy and all of them were about wide-area monitoring and control topics using Synchrophasors. WSU has put great efforts on oscillation monitoring and control and has successes to develop the relative algorithms dealing with both ambient and event measurement data from PMUs. Comparing with the perspective of frequency, this dissertation is focusing on voltage side and is to develop the effective algorithms to monitor and control the system voltages either fully or partly using Synchrophasors. These algorithms are supposed to handle ambient and event measurement data as well. Although this idea is not brand new and some methods have been developed early, the additional information beyond Synchrophasors is always required and sometimes some of them are

not fast enough. Hence, how to design the algorithms by processing the pure Synchrophasor data fast and accurately that can be truly used in real-time becomes the goal naturally.

Apparently, two tasks are contained in addressing this goal: Voltage Monitoring and Voltage Control. They are separated since voltage monitoring will assess the voltage stability which indicates the current or future states of the power systems while voltage control will maintain the voltage schedule and voltage stability by various control devices. But, they should have some relationship because they use the same data source: Synchrophasors. And this relationship should expedite the process of decision-making of voltage control with respect to the traditional SCADA and EMS ways. Nevertheless, the discussed voltage control here is mainly referring to Secondary Voltage Control whose time frame ranges from seconds to minutes. Sometimes the decision-making based on SCADA and EMS is still fast enough for on-line application which can be found in the projects done by WSU. BPA contract and Korean Electric Power Research Institute (KEPRI) contract gave us the opportunities to develop and prove several comprehensive voltage control schemes successfully, which utilizes the data from SCADA and EMS if it is available. But they also lead to the advances of the new method because the improvement is not only about time-sharing but also makes one model-free procedure turn into practical

which improves the real-time voltage control and reduces interference of model errors. Moreover, beyond the capacitors, reactors and LTC that were considered as control devices previously, SVC will be added in. For another thing, according to the fact that SCADA and EMS are still prevalent, if the algorithms related to model analysis can be developed to be the back-up of the ones from Synchrophasors, the control decision will be more redundant and reliable. Actually, this philosophy can be found through out the entire dissertation not only for the voltage control. Model analysis can still be used to verify the results of voltage monitoring from Synchrophasors.

On the other hand, the implementation interfaced with openPDC ensures the following several facts: real-time simulation, repeated verifications via different locations and different time and the ready to-go for real-time application.

1.3 Literature Review

The topic of voltage stability is receiving special attention in recent years because steadily growing loads force the grid to be operated much closer to its limits. On the other hand, the transmission networks are largely unchanged because of social and economical reasons. And the deregulation of electricity market increases the operating uncertainty. Facing these factors, operators of the electric power systems are experiencing unprecedented challenges currently.

First of all, knowing well the current voltage operating states is the key to keeping system voltages stable. The traditional and prevailing methods are almost based on SCADA and EMS, such as P-V curve, V-Q curve based analysis and the modal analysis for voltage stability including dynamic and static ways [5]. Although some on-line voltage stability assessment tools have been implemented, essentially they are still requiring the system model information and suffering from the deficiencies of SCADA and EMS. But, as Synchrophasors have been implemented widely, we have a chance to explore new ways. In fact, new applications based on Synchrophasors have occurred and been implemented across several aspects in the power systems, for example, voltage and current phasing verification, SCADA verification and back up, power system protection, oscillation monitoring. As far as voltage stability monitoring is concerned, one can find many but not vast literatures as well. WSU team proposed an algorithm and examples in [6], which proposed algorithms for quantifying the voltage instability margins in terms of reactive power loading limits by using combinations of both slow SCADA measurements and fast Synchrophasor measurements so that the critical parts of the power system in the context of voltage security in real time operating environment can be pinpointed. A synchronized-phasor-measurement-based voltage stability index was developed in [7] to determine the voltage stability margins of all system load buses but heavily depending on

network simplification limits this method in large-scale power systems. Another voltage stability index was defined in [8] to indicate the minimum one during all maximum loadability points. The basic idea of that paper was trying to find the distance (margin) between one bus and some generator nearby. However, this method only uses voltage magnitude not vector and still requires the information of the network topology as well as the status of the generators. There are many significant methods in the other papers. For example, the method of decision tree-based online voltage security assessment using PMU measurements [9], the way in analyzing and predicting the voltage stability of a transmission corridor so that the Available Transfer Capacity can be calculated [10] and the method to assess transfer stability and voltage profile stability margins which uses a more accurate PV-characteristic depending on a defined load angle instant as measured by PMUs [11]. But, the requirements such as pre-study and calculation, the information of the system topology and model simplification are necessary. And the key point is that the measured vectors are not taken full advantages.

Since we consider that PMU measurements are fast enough to provide Synchrophasors which could be treated as be continuous (30-60 measurement points per second), the measurement data during some periods have to capture some usefully system wide or local information. So the problem is how to deal with these measurement data. One

voltage-collapse criterion has been developed in [12], which considers the change in an apparent power-line flow during a time interval is exploited by using the magnitudes and angles of the local phasors. This proposed algorithm thinks of the fact that the high reactive power demand will result in the limitation of the reactive power transmission on the lines and the much closer to the critical nose and the smaller amount of reactive power can be transferred. That is, the change of the reactive power on the lines is minor. We all put the attention on the same factor which can inflect the current system status: transmission line power flows. Raczkowski and Sauer mention their idea in [13] by using transmission line power flow as well. In this paper, the Minimal Cutsets, separating a load or loads from available generation and creating an island condition if this line or lines are actually removed from service, will be found among the transmission lines in one power system. And then, a cut static transfer stability limit (CSTSL) is about to be calculated in order to predict the verticality condition of the cut complex flow trajectory. Sauer and Grijalva believed that at least one line in the system must reach an infinite line complex power trajectory which is line reactive power flow vs. line real power flow [14]. Apparently, these three authors also think of transmission line power flow as the key to assessing the system voltage stability. Moreover, for calculating CSTSL, they evaluated the partial derivative $\partial Q_{cutloss} / \partial P_{cut}$ which is compared to the total differential dQ_{line} / dV_{bus} in this thesis. But, the

proper π-model of the transmission line is required for this partial derivative while it is just optional in our algorithms.

In fact, applying transmission line power flow is not different from some the classical voltage stability assessment methods such as Continuation Power Flow (CPF). Ajjarapu and Christy invented a tangent predictor and correct method to avoid the singularity of power flow Jacobian matrix in [15]. Essentially, all of these methods are not distinct theoretically.

Secondly, the topic of voltage control is also a very important target in this dissertation because the rationality and effectiveness of the voltage control decision will directly impact the voltage stability and security after control. One realistic voltage controller should not only meet all sorts of constraints in mathematic computation but also consider the practical operation conditions and the thought of the experienced power system operators. Actually, WSU has been putting its effort on this topic for long time. Yonghong Chen proposed a discrete formulation of online voltage control scheme in [16]. This model-based controller pays primary attention to the west Oregon area of WECC system which has little generation support but many discrete devices such as capacitors, reactors and LTC transformers. The controller acts on SCADA measurements and utilizes localized power flow based on state estimator (SE) model to evaluate the incremental effects of

control device switching. The goal of this control scheme is about to keep the voltages within constraints according to several practical requirements for example: the minimum switching actions and minimum circular VAR flow. In 2002, Bonneville Power Administration (BPA) and National System Research Inc. (NSR) implemented this controller prototype. Based on this basic control strategy, Jingdong Su developed a hybrid voltage control scheme [17]. He assumed if the state estimator model maybe unavailable or unreliable because of topology errors under certain conditions, this hybrid voltage controller can evaluate control action by the local voltage estimator (LVE) which only asks SCADA measurements. Besides, the generators were considered as the main control devices when some scenarios happened. Normally, the candidate generators will reserve certain amount of reactive power output for the security purpose while they will use full reactive power output for sever situations. More generally, Jingdong Su made his design be able to handle voltage violations which occurs in several locations simultaneously by adding parallel control strategy. This is based on the fact: the big amount reactive power is hard to be transmitted along long distance and the influence of the control device is very limited out of the certain local area.

One can find the detailed explanation about the above two voltage controller in their dissertations such as the working flowchart and optimal and control constrains. This is

important and helpful to understand the Advanced Voltage Controller (AVC) presented in this dissertation. Thus, one can understand what the secondary voltage control is and where it comes from, why we choose such control and optimal constrains but the others, why such control devices have been chosen as candidates but the others, how the local power system can be formed and how many ways can do that and so on. Although, we have already gone through those literatures but it is unnecessary to re-do something which has been done before.

1.4 Summary

Motivated by the advantage of technology of Synchrophasors and their wide installation in the current power systems around world, this dissertation proposes two major applications with regard to power system voltage aspect: real-time monitoring and control, which can improve the power system voltage stability and security. Faster and more accurate voltage monitoring makes operators master the power system much better and quick and efficient control actions make the system more stable and secure.

The major contributions of this dissertation include:

1. A whole series of applications of synchrophasors: from real-time monitoring to real-time control. Comparing with SCADA, Synchrophasors will be the main data source in the future which is accurate and fast.
2. Model-free structure and corresponding methods are designed and implemented. Both structures of voltage security monitoring and control are able to work without knowledge of system models such as network parameters and phasor angles since real-time information from Synchrophasor are enough.
3. Redundant structures and methods are designed and implemented to be the back-ups of the model-free ones. These structures are model-based and act on SCADA and EMS but they are fast enough.
4. Prediction of voltage collapse is possible. Two methods are proposed to assess voltage security on-line: Fast Bidirectional Sensitivities Calculation (FBSC) and Bidirectional Linearization Approximation (BLA). The former one is totally model-free and based on PMU measurements purely while the latter one needs network parameters which are relatively constant during a long time. However, both methods are fast and accurate and can evaluate the voltage stability status and detect the weakness of the system whenever it has problems due to some stressed operating conditions or some contingencies.

5. Advanced Local Voltage Controller is developed to control the bus voltages. This controller has two parallel control structures as well: model-free and model-based. Based on the each individual framework, the corresponding local voltage predictor is used to estimate the control effects after some control device is chosen. The crosscheck is designed simultaneously so that the large difference between them can be found. Moreover, the control action is of optimization because certain practical and feasible objective function is utilized to select the final decision among many choices.
6. A prototype of on-line voltage security monitoring tool is implemented with C# and works within openPDC.

The remaining parts of this dissertation are organized as follows. Chapter 2 defines the Global Voltage Stability Assessment Index which is the key to indicate the level of corresponding bus voltage stability. This chapter mainly focuses on proof and comparison theoretically. Thus, the static power flow model will be utilized to study and validate this global VSA index by comparing with the other typical voltage stability methods. In the meanwhile, a fast computation method to calculate this global VSA index and its testing will be presented in this chapter as well. And, the definition of the line sensitivity will occur first in Chapter 2 but will be fully taken advantage in Chapter 3 since two methodologies will be developed to apply Synchrophasors to attain line sensitivity and

then the global VSA index. These ways can be model-free but the back-up design with requirement a little of system model information will also be provided. A number of tests via real-time PMU measurements will be shown in this chapter to prove the validation of these two methodologies. Chapter 4 targets on representing the topic of the real-time voltage control. Each detail could be found, such as the primary model-free Local Voltage Predictor, the back-up model-base Local Voltage Predictor and the formulation of the voltage control scheme. A few of primary tests are committed as well. In the last chapter, the conclusion of this dissertation are summarized and important future work will be indicated.

Chapter 2

The Global Voltage Stability Assessment Index and Line Sensitivity: Fundamental Concept and Fast Computation Via Power Flow

For any electric power system, its static power flow model is always crucial and is the basis for analyzing all sorts of its states even for dynamic analysis. Although the computation time could be an issue for on-line or real-time application sometimes or somewhere, this methodology can give us areawise as well as global results. Consequently, the successful proof to one idea in power flow way must be more convincing. On the other hand, since there are many classical methods in power flow analysis, we can easily compare the results from our designs with those from the classical methods so that the verification will be enhanced. This chapter defines a new global index to assess system voltage stability. With the help of the standard definition of power flow model, this index will be proven theoretically. And then, for computation purpose, that is, based on the common and available information from standard power flow, one method is developed to

access this index without consuming much time. Although, this computational way is not truly realistic for real-time assessment with contrast to the methods represented in the next chapter, it is still progressive. Further, all the conclusions will be supported by tests on several standard test systems.

2.1 The Line Sensitivity and Computation Method

As for one electric power system, one typical connection with two-ending buses and one transmission line or equivalent line model is shown in Fig 2.1. Assume that bus i is PQ type bus and has the line real power flow P_{ij} and Q_{ij}.

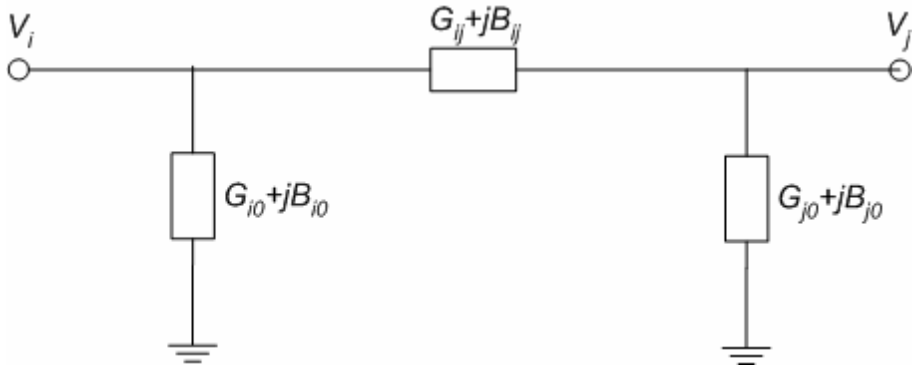

Figure 2.1 One connection model with two buses and one line

Thus, the basic line power flow equations are:

$$P_{ij} = V_i^2(G_{ij} + G_{i0}) - V_iV_j(G_{ij}\cos\delta_{ij} + B_{ij}\sin\delta_{ij}) \tag{2.1}$$

$$Q_{ij} = -V_i^2(B_{ij} + B_{i0}) - V_iV_j(G_{ij}\sin\delta_{ij} - B_{ij}\cos\delta_{ij}) \tag{2.2}$$

Where $\delta_{ij} = \delta_i - \delta_j$ is the difference between two bus voltage angles. As far as the bus voltage is concerned, the most attention will be paid to the reactive power in small region around normal operation point. Using Taylor's equation for (2.2), we have:

$$\Delta Q_{ij} = \Delta Q_{ij}(\Delta V_i, \Delta V_j) = \frac{\partial Q_{ij}}{\partial V_i}\Delta V_i + \frac{\partial Q_{ij}}{\partial V_j}\Delta V_j + O(V_i, V_j) \tag{2.3}$$

Then, the line sensitivity with regard to bus i is defined as below:

$$\varphi_i = \frac{\Delta Q_{ij}}{\Delta V_i} = \frac{\partial Q_{ij}}{\partial V_i} + \frac{\partial Q_{ij}}{\partial V_j}\frac{\Delta V_j}{\Delta V_i} + \frac{O(V_i, V_j)}{\Delta V_i} \tag{2.4}$$

We are considering the relationship between the line reactive power and that bus voltage. For one thing, the change of the line reactive power could lead to the change on that bus voltage. For another, the reverse fact is always true. As the matter of fact, these changes are also coupled with the other ending bus, which is the reason that $\partial Q_{ij} / \partial V_i$ cannot be appointmented to be the line sensitivity. Let us see what $\partial Q_{ij} / \partial V_i$ is standing for. From (2.2),

$$\frac{\partial Q_{ij}}{\partial V_i} = -2V_i(B_{ij} + B_{i0}) - V_j(G_{ij}\sin\delta_{ij} - B_{ij}\cos\delta_{ij}) \tag{2.5}$$

In the realistic operation area, the bus voltage is approximately close to 1 p.u. and is much smaller than the values of the equivalent line parameters so that the contribution of line is dominant in calculating $\partial Q_{ij} / \partial V_i$. Therefore, $\partial Q_{ij} / \partial V_i$ is relatively stable and constant and

cannot reflect the truly state of the bus. But, the proposed line sensitivity $\Delta Q_{ij} / \Delta V_i$ will not have these issues because the changes of the bus voltages from both endings will be considered at the same time.

Naturally, there is one way to attain the proposed line sensitivity φ_i by calculating partial derivatives of the line reactive power flow Q_{ij} with respect to V_i and V_j and by omitting the high order terms without big errors. But, there is a much simpler and straightward method of accessing line sensitivity φ_i , which is about to measure the variations of Q_{ij} and V_i in one small region simultaneously. That is, directly calculating the left hand side of the secondary equal sign in (2.4) means any piece of change on both endings of one line will be taken account into. So, this approach has at least two advantages: i) Calculation is simple; ii) The effects not only from the bus voltage at bus i but also from other factors are also considered. When the two endings of this line are PQ buses, V_i's changing must lead to the change of V_j. For some conditions, especially the real power injection changes, this similar process can result in the changes of bus angles, however, these changes are minor in most conditions.

For one certain power system, if two power flow cases in one operating condition are available, the line sensitivity for each PQ bus can be achieved easily. On the other hand, for study purposes, one base case can be used to calculate the line sensitivities. In one small

and acceptable region, the change of the load at bus i can provide the satisfied ΔQ_{ij} and ΔV_i. We can simulate this process of load changing simply by inserting a reasonable amount of shunt capacitor/reactor at bus i and then solving the power flow.

2.2 The Global Voltage Stability Assessment Index

This global voltage stability assessment index for bus i is defined as below:

$$\Gamma_i = \frac{\Delta Q_{Li}}{\Delta V_i} = \frac{\sum_j \Delta Q_{ij}}{\Delta V_i} = \sum_j \frac{\Delta Q_{ij}}{\Delta V_i} \tag{2.6}$$

Here ΔQ_{Li} is the variance of the load at bus i and ΔV_i is the corresponding change of that bus voltage. For any PQ bus, all loads are supported by the power coming from transmission lines and the other series equipments, so the voltage stability of that bus can be represented according to the summation of all line sensitivities for that bus.

The straightforward and simple explanation for this definition is that this global VSA index is similar with the slope of that operating point at Q-V curve. Purely, as the load rises, the bus voltage will drop to the collapse point and the slope will approach the “zero”. This fact was mentioned in other way in [1] where Kundur said the slope of V-Q curve will be infinite at the collapse point. Hence, the similar process can demonstrate that this global VSA index is able to indicate the level of the bus voltage stability.

The power system linearized equations can be expressed:

$$\begin{bmatrix} \mathbf{\Delta P} \\ \mathbf{\Delta Q} \end{bmatrix} = \begin{bmatrix} \mathbf{J_{P\theta}} & \mathbf{J_{PV}} \\ \mathbf{J_{Q\theta}} & \mathbf{J_{QV}} \end{bmatrix} \begin{bmatrix} \mathbf{\Delta \theta} \\ \mathbf{\Delta V} \end{bmatrix} \tag{2.7}$$

Assume $\mathbf{\Delta P = 0}$ for Q-V analysis. Then the induced system equation is:

$$\mathbf{\Delta Q} = \left[\mathbf{J_{QV}} - \mathbf{J_{Q\theta}} \mathbf{J_{P\theta}^{-1}} \mathbf{J_{PV}} \right] \mathbf{\Delta V} = \mathbf{J_R} \mathbf{\Delta V} \tag{2.8}$$

$\mathbf{J_R}$ is the induced Jocobian matrix. So the solution could be:

$$\mathbf{\Delta V} = \mathbf{J_R^{-1}} \mathbf{\Delta Q} = \frac{\mathbf{adj(J_R)}}{\mathbf{det(J_R)}} \mathbf{\Delta Q} \tag{2.9}$$

where $\mathbf{adj(J_R)}$ is the adjoint of $\mathbf{J_R}$ and $\mathbf{det(J_R)}$ is the determinant. Since $\mathbf{\Delta Q} = [0 \quad \dots \quad \Delta Q_i \quad \dots \quad 0]$, we can have:

$$\frac{\Delta V_i}{\Delta Q_i} = \frac{[\mathbf{adj(J_R)}]_{ii}}{\mathbf{det(J_R)}} \tag{2.10}$$

or

$$\frac{\Delta Q_i}{\Delta V_i} = \frac{\mathbf{det(J_R)}}{[\mathbf{adj(J_R)}]_{ii}} \tag{2.11}$$

When the system approaches to the critical node, the determinant of induced Jocobian is changing smaller and smaller, meanwhile the value of (2.10) will become larger and larger while that of (2.11) does smaller and smaller. Because of the singular Jocobian matrix,

theoretically, $\Delta V_i/\Delta Q_i$ should be infinite. Correspondingly, $\Delta Q_i/\Delta V_i$ is "zero". Thus, $\Delta Q_i/\Delta V_i$ (Γ_i) can be one indicator of the system voltage stability.

But we have to pay attention to the more comprehensive fact. As we know, except the saddle node bifurcation, the complementary limit induced bifurcation is still very common case. The purposed VSA index should has ability of handling such cases also. As to the complementary limit induced bifurcation case introduced in [18], right after some bus changes from PV type to PQ type, the new induced problem is suddenly unstable. That is, the determinant of the older induced Jocobian is smaller value but that of the new one is of different sign [18]. In other words, $\Delta Q_i/\Delta V_i$ will stop at some small value instead of zero. This will be illustrated in the following comparison.

Fig 2.2 and Fig 2.3 show these two bifurcation cases in Q-V curves and the index vs. Q. Fig 2.2 is for bus 12 in New England 39-bus system. This is a saddle node bifurcation. At the critical node of Q-V curve, the tangent of critical node of Q-V curve is almost vertical. Correspondingly, Γ_{12} is 1.18 which is very close to "0". Fig 2.3 is a complementary limit induced bifurcation case from IEEE 300-bus system. For bus 14, the power flow fails when its reactive load is approximately 470 MVAR. From Q-V curve, the slope around the critical node is apparently not infinite. This result is reflected very well on the value of Γ_{14} which is 7.01.

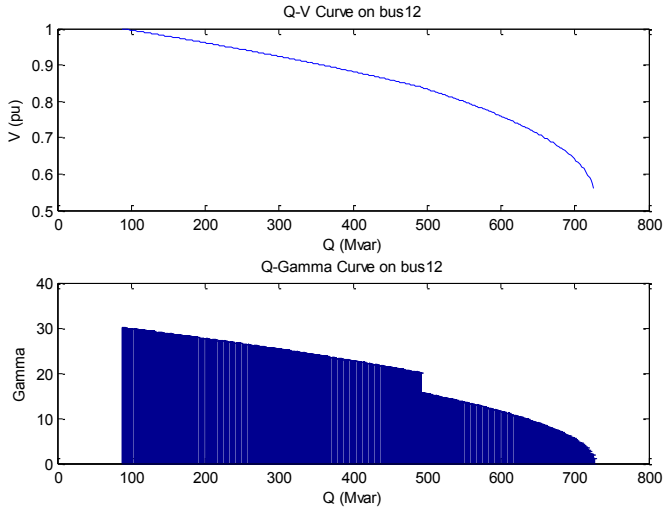

Figure 2.2 Saddle node bifurcation from New-England 39-bus system

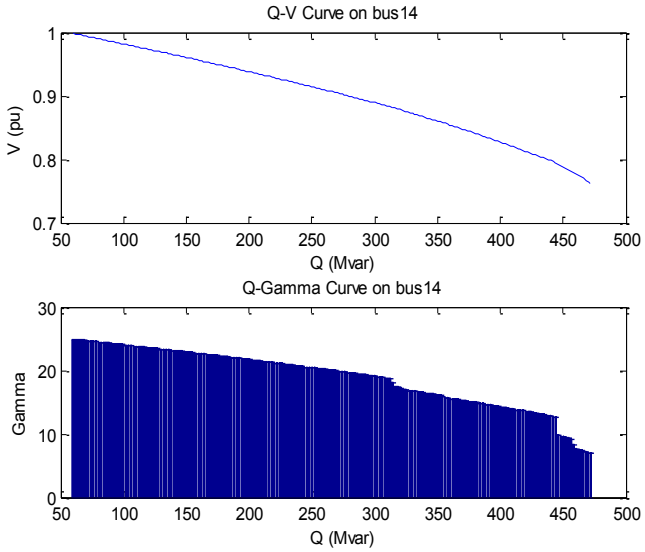

Figure 2.3 Complementary limit induced bifurcation from IEEE 300-bus system

It is obvious that the index and the Q-V curve match well with each other. This conclusion is also valid even for the lower portion of Q-V curve. Namely, the Γ_i will

change the sign after the power solution passes the critical node and still has the same trend as that of lower portion of Q-V curve in the mean of continuation power flow. Since this situation is not realistic and unstable, the results about lower portion are not shown in the above figures.

Naturally and consequently, we conjecture the following rules only using this global index Γ_i to assess the system voltage stability at any PQ bus i.

The index Γ_i can assess bus voltage security by its value and the statements:

i) ***A "high" value of Γ_i indicates a "strong" bus in terms of being distant from static voltage instability limit.***

ii) ***If there is any bus with Γ_i value near "0", the system is close to static voltage stability limit related to saddle-node bifurcation, and the bus with the lowest Γ_i is likely the critically voltage stressed part of the system.***

iii) ***If one system has the bus whose Γ_i is less than some critical value, and then the system may be vulnerable towards voltage stability caused by either of saddle-node or limit induced bifurcations. We need to pay attention to this system voltage security.***

Statement (iii) is related to complementary limit bifurcation cases where small number may came up from simulations on numerous cases and various systems. Essentially, bigger value means more conservative and the smaller one could make control actions too late to re-stabilize this system. In other words, *no matter which bifurcation the system will encounter, the system is operating in voltage unsecure region and needs to be controlled if some bus has too low* Γ_i. In the next section, this rule is applied to assess several power systems so that the validation of this rule can be proven again.

2.3 Case Studies

IEEE 9-bus system, IEEE 30-bus system, New England 39-bus system and IEEE 300-bus system will be employed as the test systems in this section. One can find the case data from the MATPOWER Package [19]. And the MATPOWER is the engine to solve the power flow as well. First, we calculate the index Γ_i of each bus for each system. And then the system voltage stability level will be known in term of the proposed rules. In order to confirm the conclusions, Q margin at each bus i is calculated. That is, if the weakest bus whose Γ_i is minimum will have minimum Q margin, statement (i) is confirmed. Simultaneously, by checking the region where the value of Γ_i locates, we will know how far the system is from the collapse. For contingency analysis, we choose some line to be tripped and calculate the Γ_i after the contingency to see how the index performances and what information it can carry out.

2.3.1 VSA Index from Base Case

Each PQ bus in each test system will have its own VSA index. Although one load change is enough by inserting a small amount of capacitor/reactor at that bus for one local sub-system subject to the big systems, one inserting action will be done at each bus in each test system in order to get more accurate VSA index and mitigate the affect from control action during the power flow calculation. In the following graphs, the horizon axis is

representing bus numbers in that test system which can be found in Appendix A while the vertical axis is showing the VSA index with the "absolute" value (means no unit like MW or MVAR) for that bus.

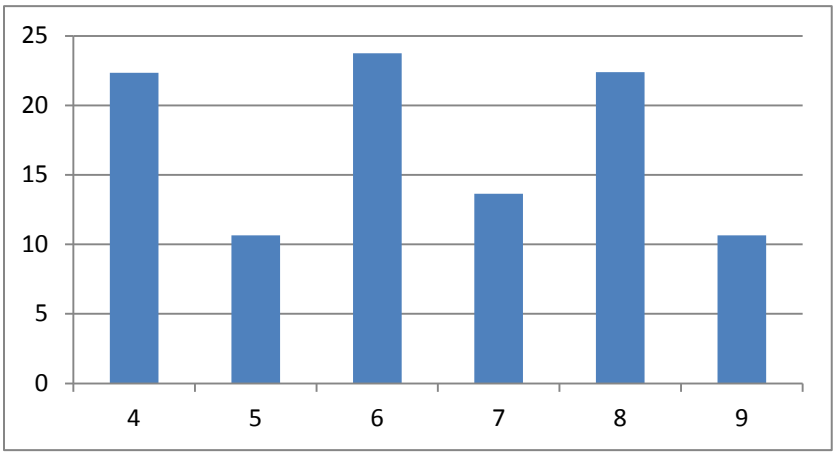

Figure 2.4 The index Γ_i in IEEE 9-bus system

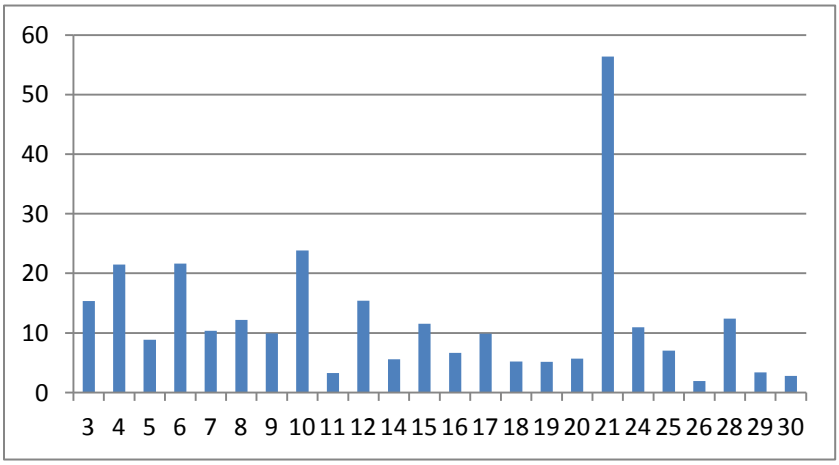

Figure 2.5 The index Γ_i in IEEE 30-bus system

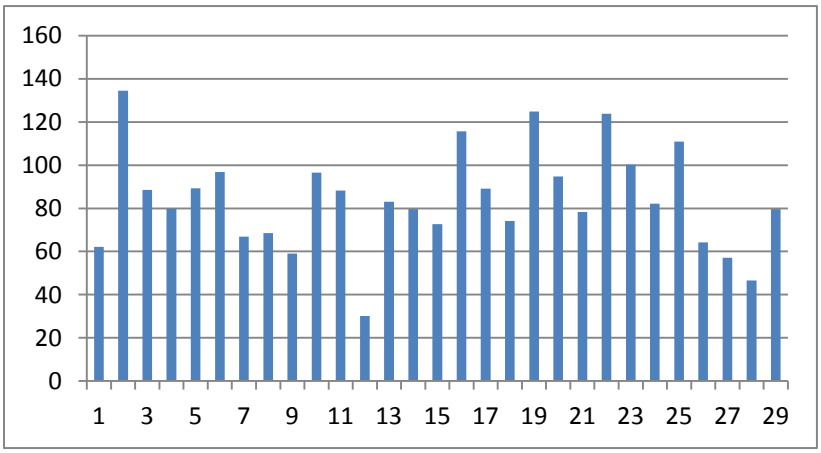

Figure 2.6 The index Γ_i in New England 39-bus system

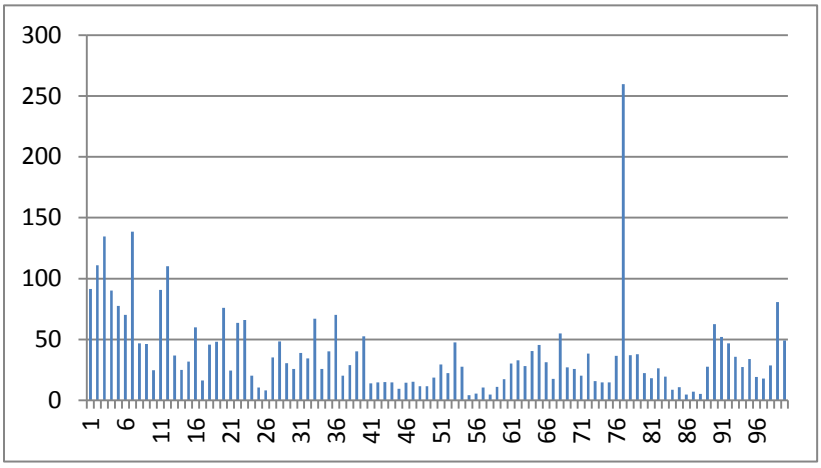

Figure 2.7 The index Γ_i in IEEE 300-bus system (bus number 1-127)

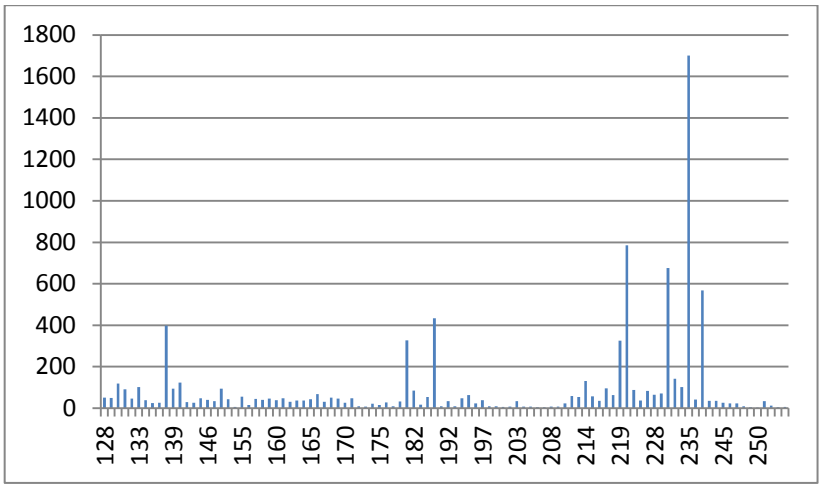

Figure 2.8 The index Γ_i in IEEE 300-bus system (bus number 128-322)

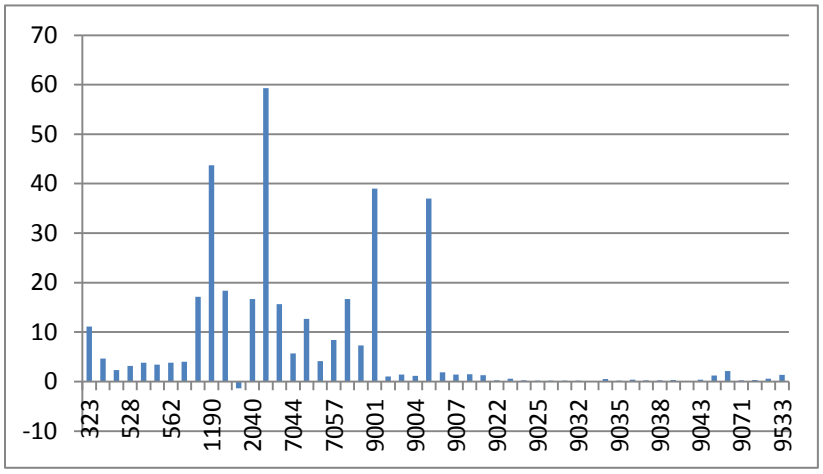

Figure 2.9 The index Γ_i in IEEE 300-bus system (bus number 323-9533)

By the indices and the proposed statements, the weakest bus in each system is:

- **9-bus system: Bus 9.**
- **30-bus system: Bus 26.**
- **39-bus system: Bus 12.**

- **300-bus system: Bus 9042. (There is a negative Γ_i. This is a not typical fact and will be explained in the next section).**

Moreover, 30-bus system and 300-bus system are not secure since the minimum Γ_i in these two systems are very close to zero.

2.3.2 The Comparison between VSA index and Q margin

From the base case and assuming that the active power is constant, we increase reactive loads gradually at each bus individually until the power flow solution fails. The index and Q margin are put into one graph to show the relationship between them visually. The left y-axis is the Q margin in MVAR while the right y-axis is about the indices. Also, the weakest buses resulting both from the VSA index and from Q margin are put together into one table so that one can easily find they are identical. We are trying to do this comparison on the strongest buses (the maximum Q margin and the biggest VSA index), the current proposed statements have not been extended to this yet since more complicated factors could be dominated.

a. 9-bus system: Table 2.1 and Fig 2.10.

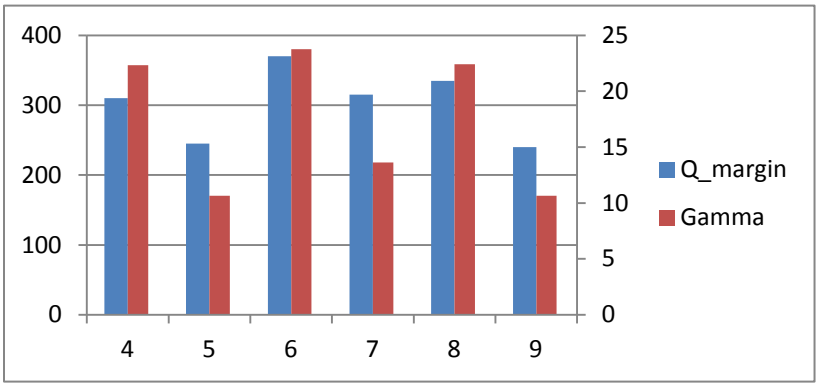

Figure 2.10 The comparison between Γ_i and Q margin for 9-bus system

	Minimum	Maximum
Index	**Bus 9:10.639**	Bus 6:23.753
Q margin	**Bus 9:240 MVAR**	Bus 6:370 MVAR

Table 2.1 Weak and strong buses in 9-bus system from index and margin

b. 30-bus system: Table 2.2 and Fig 2.11

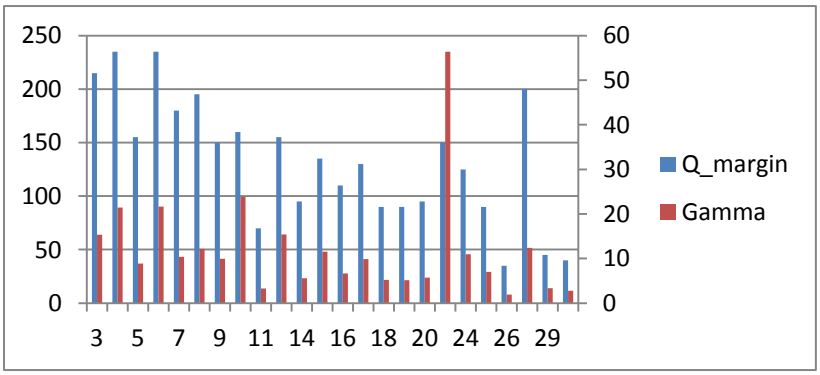

Figure 2.11 The comparison between Γ_i and Q margin for 30-bus system

	Minimum	Maximum
Index	**Bus 26:1.952**	Bus 21:56.399
Q margin	**Bus 26:35 MVAR**	Bus 4:240 MVAR

Table 2.2 Weak and strong buses in 30-bus system from index and margin

c. 39-bus system: Table 2.3 and Fig 2.12

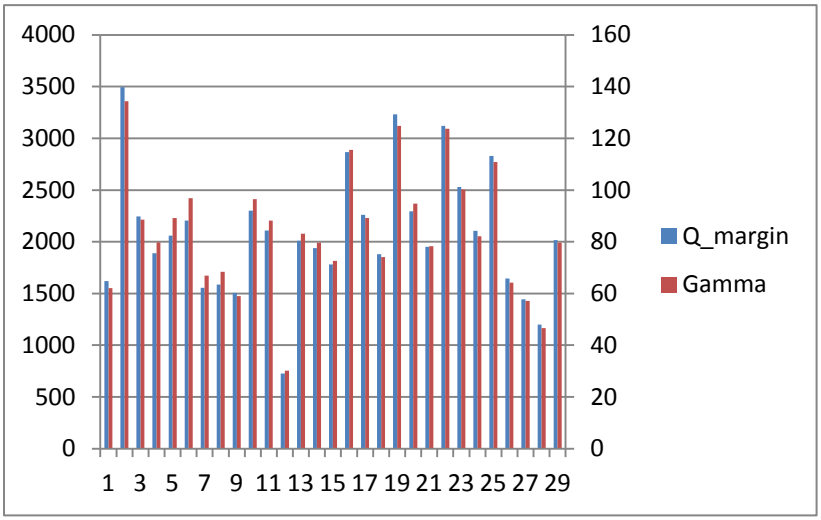

Figure 2.12 The comparison between Γ_i and Q margin for 39-bus system

	Minimum	Maximum
Index	**Bus 12:30.208**	Bus 2:134.37
Q margin	**Bus 12:725 MVAR**	Bus 2:3495 MVAR

Table 2.3 Weak and strong buses in 39-bus system from index and margin

Note that we use this exact case in MATPOWER Package. The generator reactive power limit is -9999 to 9999. So we have so big Q margin.

d. 300-bus system: Table 2.4 and Fig 2.13 to Fig 2.15

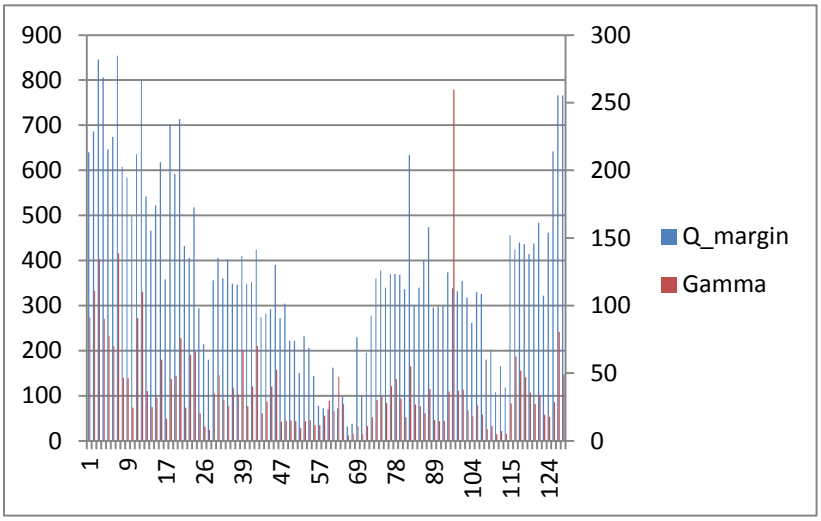

Figure 2.13 The comparison between Γ_i and Q margin for 300-bus system (1-127)

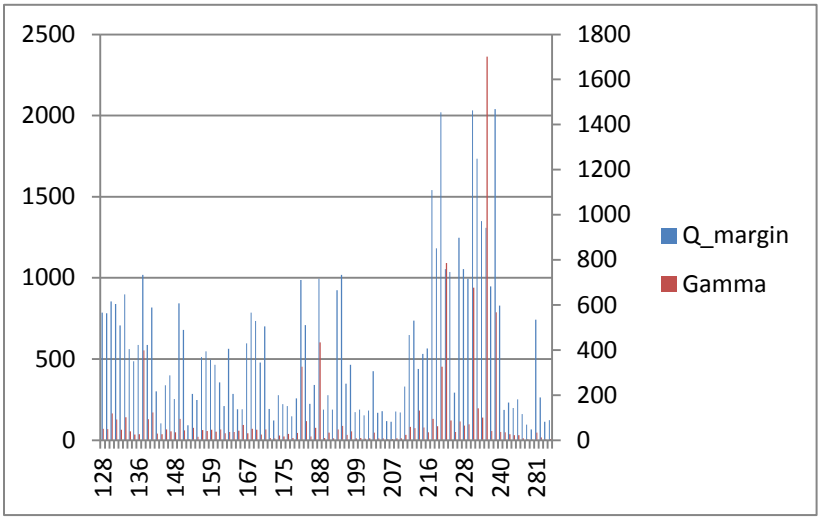

Figure 2.14 The comparison between Γ_i and Q margin for 300-bus system (128-322)

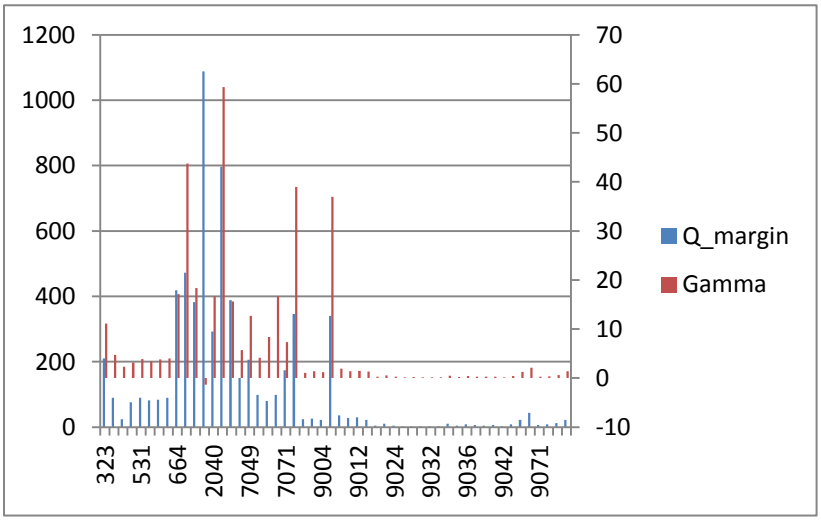

Figure 2.15 The comparison between Γ_i and Q margin for 300-bus system (323-9533)

	Minimum	Maximum
Index	**Bus 9042:0.1573**	Bus 235:1701.21
Q margin	**Bus 9042:2 MVAR**	Bus 237:2040 MVAR

Table 2.4 Weak and strong buses in 300-bus system from index and margin

There are two points we have to explain.

i) The maximum index 1701.21 at bus 235 seems abnormal but it is correct because bus 235 is very close to a generator (bus 238). In current operating conditions, that bus voltage changes very small since it is controlled by the generator. If the reactive load is increased by 100 MVAR, the index becomes 119.28. Except this bus in current situation, the maximum one is 785.933 at bus 223.

ii) That negative index -1.372 at bus 1201 is not treated as the minimum one because this scenario is not typical. This negative value means more Q loading results in the bigger bus voltage. The exact reason is that one of two lines has *0 resistance and negative reactance*, which makes this line act as serious capacitor. We only find one such case through all base cases even if we calculate the indices on the East Europe 2736sp system [19].

Although these two factors exist, they do not have any effect on these conclusions. The bus with the minimum index has the minimum Q margin in the same time. Very small indices reveal the systems are not secure and even face the collapse.

2.3.3 Examples on Line Tripping

Line tripping is related to topologic change of the system. Normally, tripping out one transmission line with high power flows would make system weaker. Since the weakest bus represents the system voltage security, the minimum index value should become smaller when the system becomes weaker. This process can happen to the different bus. That is, the weakest bus can be shifted from one bus to the other before and after line tripping.

30-bus system and 300-bus system are not suited to be the cases for this contingency since the base cases are already stressed and so close to the collapse point. On the contrary, 39-bus system looks very stable. So this test system can be the good example to show this scenario, however, the same process can be done on any other systems and there is no difference to reveal the true.

First contingency is that the line between bus 15 and bus 16 is tripped out. Second contingency is to trip out the line between bus 28 and bus 29. The results are shown in Fig 2.16.

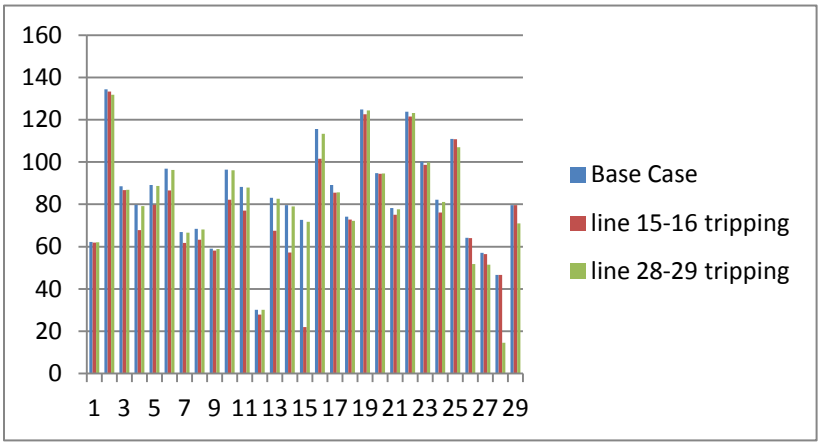

Figure 2.16 The index Γ_i from base case and contingencies

The first contingency made the weakest bus be bus 15 while it became bus 28 after line 28-29 tripping out. The reason is simple. For the loads at bus 15 and bus 28, we cut one of two major feeding lines so that the system naturally becomes weaker. On the other hand, the minimum Q-margin is 455 MVAR at bus 15 after first contingency and 345 MVAR at bus 28 after second contingency which corroborate the conclusion from the VSA index once again.

2.3.4 Examples on Load Increasing

When the load is getting higher, the system operational reliability status becomes worse and worse. Therefore, the system will lose voltage stability naturally. If this situation happens at one bus, the index of that bus will become smaller. If this situation happens at a region or whole system, the indices in that region or all indices also become smaller. We verify this fact by the 30-bus system.

The original load amount is not big even in base case. We increase the load at bus 7 by 300%, that is, $P_L = 22.8 \rightarrow 91.2$ MW and $Q_L = 10.9 \rightarrow 43.6$ MVAR. The comparison is shown in Fig 2.17.

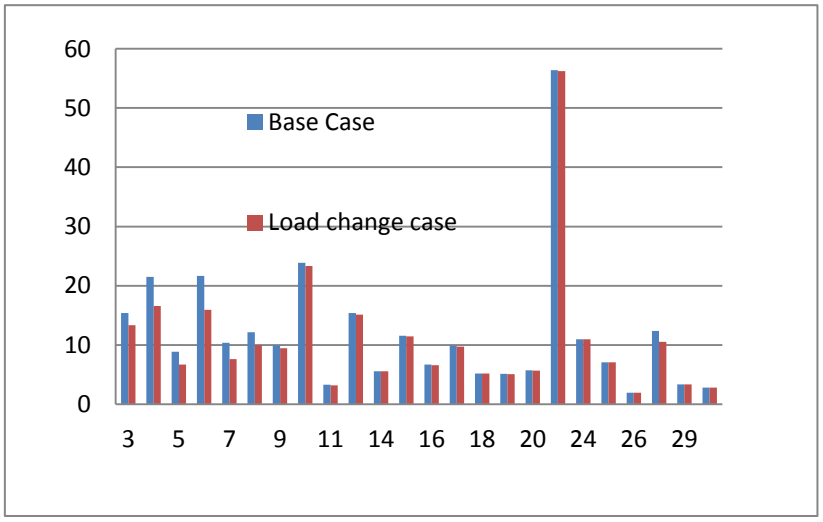

Figure 2.17 The index before and after increasing load at bus 7

It can be seen that those buses (bus 3,4,5,6 and 8) in the neighbor of bus 7 are having obvious impacts while those far way from bus 7 have not. But as a whole, the indices decline without any particular excuse.

The 30-bus system is also a stressed test system. Remember that the minimum index is 1.9522 at bus 26. Although the total real and reactive power in base case are only 189.2 MW and 107.2 MVAR, only 50% increasing at all buses from the original ones, can drive the system close to the collapse point. And then we will see the observable declines for all indices in Fig 2.18.

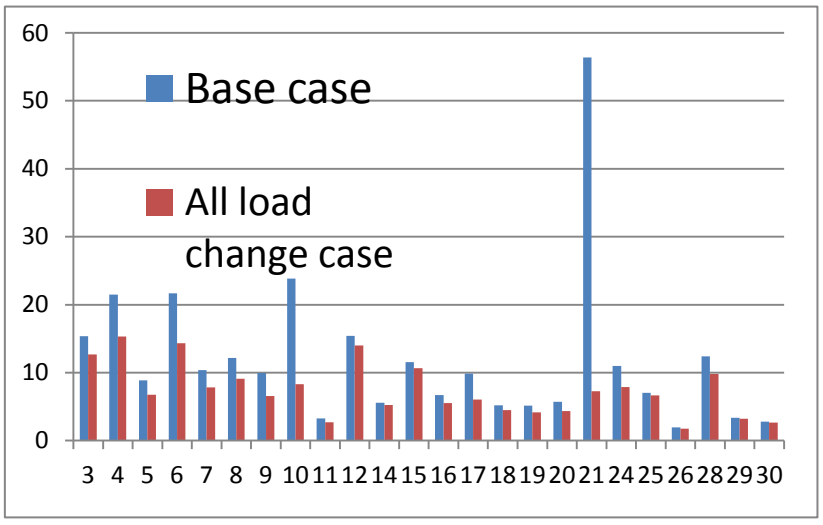

Figure 2.18 The index before and after load increasing at all buses

All indices have decreased after load increasing and meanwhile some big indices change dramatically. That is, the whole system is too weak to endure big changes. In fact, only 15%

more load increasing will make this system collapse. Considering the original amount of the load, this number is not surprising.

2.4 Summary

This chapter defines a new global voltage stability assessment index to assess system voltage stability and security. The VSA index of each bus consists of all line sensitivities connected at that bus. Theoretically, the line sensitivity is the total differential of line reactive power versus the corresponding bus voltage. In a small region, $\Delta Q_{ij}/\Delta V_i$ is used to replace that total differential without unacceptable error. Since all power transfers occur through transmission lines or equivalent lines and this VSA index has capacity of gathering all information from line sensitivities, it can represent that bus voltage state of stability and security. This index is similar to the slope of certain point on V-Q curve or the degree of stability in static analysis about voltage stability study. By checking the minimum index in one system at some operation condition, the weakest bus can be easily found. Meanwhile, the level of system voltage stability can be estimated, such as whether the system is close to certainly critical limit. It can be used to mark the impact which a contingency or load change gives as well. All valuable conclusions are summarized into the practical rules to assess system voltage stability already.

A fast computation method based on power flow is proposed to attain line sensitivity. This method simulates the load change at some bus by inserting a reasonable amount of shunt device to capture V and Q changes. Although this method needs power flow calculation, the process is simple and not time-consuming.

The VSA indices and the related rules are tested on four typical test systems: IEEE 9-bus system, IEEE 30-bus system, New England 39-bus system and IEEE 300-bus system. Thus, those rules based on this index are proven to be effective and all judgments from the rules are consistent with those from the other voltage stability assessment methods.

Chapter 3

Real Time Voltage Stability Monitoring: Estimation of The Global VSA Index And Line Sensitivity Using Synchrophasors

In the last chapter, the defined global VSA index and the proposed rules are proven to be very useful to assess the voltage stability. As far as the real time application of this design is concerned, more practical and faster way to access the VSA indices is the key. That is, if we can attain line sensitivity quickly and accurately, we will have a powerful tool to evaluate the current system status and more. This chapter provides two methodologies which are able to estimate line sensitivity purely from Synchrophasors: Fast Bidirectional Sensitivities Calculation (FBSC) and Bidirectional Linearization Approximation (BLA). These two methodologies can deal with the most common data format of Synchrophasors by several important processes, such as Data Split and Weighted-Average-Slope so that the data set looking like disordered will show the useful information eventually. The distinction between FBSC and BLA is that FBSC directly calculates line reactive power and find every piece of change for both V and Q while BLA can achieve the results by

approximating the changes of line reactive power flow in terms of its linearized equation. So, BLA needs impedance values for the line. Meanwhile, Jump if occurring in the measurement can be a good reference to the results from FBSC and BLA and help tuning the thresholds because of its special attribute. For more understanding of these procedures, this chapter also explains why the Synchrophasors are showing in this disordered way and the possible causes, what the bidirectional means and what Jump is. These two methodologies are tested successfully by both the repeatable and accessible simulation Synchrophasors and real Synchrophasors. Further, the results from two algorithms are comparable and practical. For the demonstration of real time application, a snapshot of results from field measurements is shown as well.

3.1 Preparation

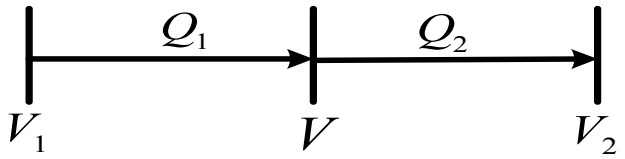

Figure 3.1 A common model from power systems

Fig 3.1 shows a most common model from power systems, which can be a piece of the big topology and can be anywhere in the whole system. Notice, this is just simplified model. In the real system, every bus can be simplified into the above one by integrating the

line reactive power injections and outgoings. Here Q_1 and Q_2 are the line reactive powers seen from the middle bus with voltage V. Before we do the further introduction, two phenomena have to be stated and explained since they are important for readers to understand the entire design. Now, we have the following two typical phenomena in power systems:

Phenomenon 1: The V change can lead to the V_1 change and V_2 change. On the other hand, if the change is coming from V_1 or V_2, then V will be changed as well.

This is always true when one bus voltage responses naturally the other changes. But, if some bus is "remoter control bus", the situation could be different. Here, we think all buses responses naturally unless they are noticed particularly.

Phenomenon 2: No matter when V increases or decreases, Q_1 or Q_2 will respond this V change and then it could be increasing or decreasing. Also, the opposite process is the fact. That is, $\Delta V > 0$ does not certainly mean $\Delta Q_i > 0\ (i = 1,2)$. And in the opposite way, $\Delta Q_i > 0\ (i = 1,2)$ does not certainly mean $\Delta V > 0$.

The following scenarios can demonstrate truth of this phenomenon. In the usual situations, if V_1 increases, then $V(V_2)$ will increase and $|\Delta V_1| > |\Delta V| > |\Delta V_2|$. Consequently, Q_1 and Q_2 will increase such as $\Delta Q_1 < 0$, $\Delta Q_2 > 0$ and $|\Delta Q_1| = |\Delta Q_2|$ if the loss is not considered. On the other hand, if V_2 increases, then $V(V_1)$ will increase and $|\Delta V_2| > |\Delta V| > |\Delta V_1|$. Consequently, Q_1 and Q_2 will decrease such as $\Delta Q_1 > 0$, $\Delta Q_2 < 0$ and $|\Delta Q_1| = |\Delta Q_2|$. Once more, if V increase originally, then we have no doubt about the fact that both V_1 and V_2 response to rising. $\Delta Q_1 > 0$, $\Delta Q_2 > 0$.

Listing all situations is trivial but unnecessary since the power system is so complicated that sometimes the causality of the change is blurry. However, we are successful to describe the existences of the positive and negative slopes when the above two scenarios occur in power systems. In other words, the φ_i defined in (2.4) for the middle bus with voltage V can be positive or negative when V changes. Moreover, in most time, the φ_i doesn't always show one sign all the time. In fact, since the buses are coupled among them and all kinds of factors result in the changes of their states, it is hard to distinguish which one is dominated during one period. Hence, the immediate influence will make us barely observe the curves with purely positive or purely negative slopes during that period. A number of positive and negative slopes mix up with each other so that the whole plot of V_i

vs. Q_{ij} looks disordered and useless. But, if we are able to separate them back into two sets in some ways again, and then the situation will be totally different. Synchrophasors gives us such an opportunity because the sufficiently fast and accurate measurements are available, hence we can have piece by piece information of the buses' status. That is, we can have one small time-period during which the purely positive slopes or the purely negative slopes are only contained by the V-Q curve.

In terms of this basic idea, the designs in the following section will become more rational.

3.2 Basic Scenarios

For better describing that the mixture of positive slopes and negative slopes during some period, we shall call it to be "fluctuation". And, simply but not insufficiently, only four basic scenarios are able to summarize this fluctuation.

i. Q_1 *and* V *change in the same directions.*

Regardless of the original change coming from the line reactive power or bus voltage, we always have the plot as the one in Fig 3.2a. V' is the current operation point and remember Q_1 is negative since it is injection with respect to the bus V.

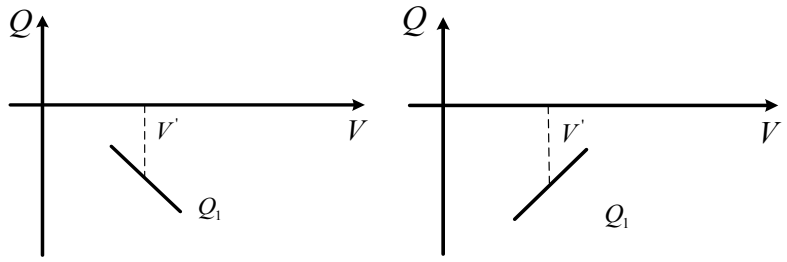

a b

Figure 3.2 The V-Q curve for injection line power in one small interval

ii. Q_1 *and* V *change in the opposite directions.Fig3.2b.*

iii. Q_2 *and* V *change in the opposite directions.Fig3.3a.*

iv. Q_2 *and* V *change in the opposite directions.Fig3.3b.*

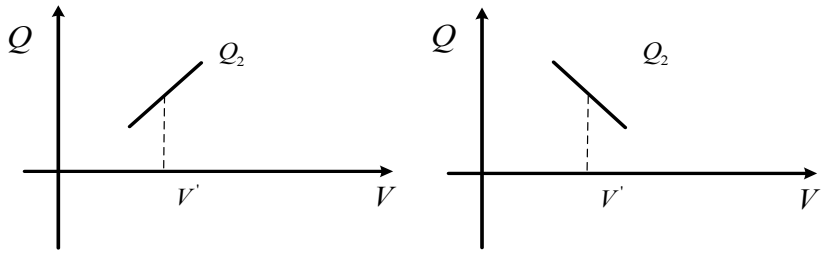

a b

Figure 3.3 The V-Q curve for outgoing line power in one small interval

Now, it is easy to illustrate that during one time period, such as several seconds or minutes, the numeric amount of plots in Fig 3.2a and those in Fig 3.2b could overlaps with

themselves or with each others. The same situation can happen to the plots in Fig 3.3a and 3.3b as well. Then the so-called “fluctuation” is formed by the combination of those plots. For example, Fig 3.4 represents simple one among the vast combinations. Notice that the real curves are not orderly like this and the shapes are only for case. In the next section, the real fluctuation from real Synchrophasors will be shown.

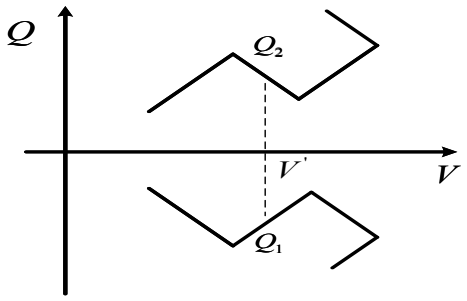

Figure 3.4 One virtual case for V-Q fluctuation

3.3 Analysis on Synchrophasors: Basic Steps For FBSC and BLA

Moving from last chapter, now we are handling the actual Synchrophasors from real power systems. So we could encounter the same problems as the other data mining or processing has. Fortunately, the current PMU equipments have the capacity to cope with the most common situations and then the data from PDCs is ready to be used. Since our designs do not handle the raw data directly from PMU equipments, after studies on plenty

of Synchrophasors from PDCs, we build three essential steps to deal with these data in order to ensure we can attain trusted results.

In the next sub-sections, the necessity for each step will be discussed by analyzing the cases from actual Synchrophasors. Here, we do not show the locations where the Synchrophasors come from by Honor Non-Disclosure Agreement(NDAs).

3.3.1 Data Filter

Bad data points are always troublesome. Fig 3.5 shows very typical measurements from PMUs during a certain time-frame.

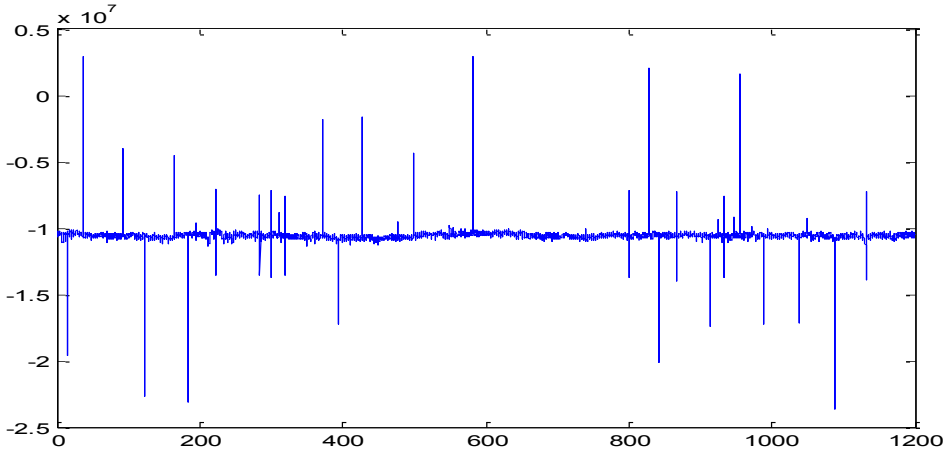

Figure 3.5 The line reactive power from PMUs during 20 minutes

Many odd measurement points occurred in this time-plot. It is not practical and not true for those points where the line reactive power changed so much first and then changed back at the next moment. In fact, we do not care about what made this behavior happen. But, definitely, this so big variance of line reactive power is not meaningful and will drive the calculation of the differential of Q_{ij} far away from the right aspects. Like bad measurement points, the other consideration is about no measurement during some period, which is also common and has the similar influence when we calculate the line sensitivities. The efficient way to solve this problem is to set some thresholds to eliminate such points from the whole data sets. Generally, these thresholds should include values for voltage magnitude and current magnitude. And this process is not complicated but those proposed thresholds need to be tuned when the special power system is concerned.

For another, the high-frequency noise seems not to be our issue now because its magnitude related to the voltages and currents is minor. Besides, the entire analysis is in time domain.

3.3.2 Data Split

Since the fluctuation is the mixture of positive and negative slopes, which appears useless for the further analysis in this expression, we have to figure out some method to

overcome this defect. Then, Data Split is just a way to convert the curves like Fig 3.4 back into two sets with the purely positive or negative slopes like Fig 3.2 or Fig 3.3. Let us see an example from actual Synchrophasors from the Eastern Power System in United States. See the Fig 3.6.

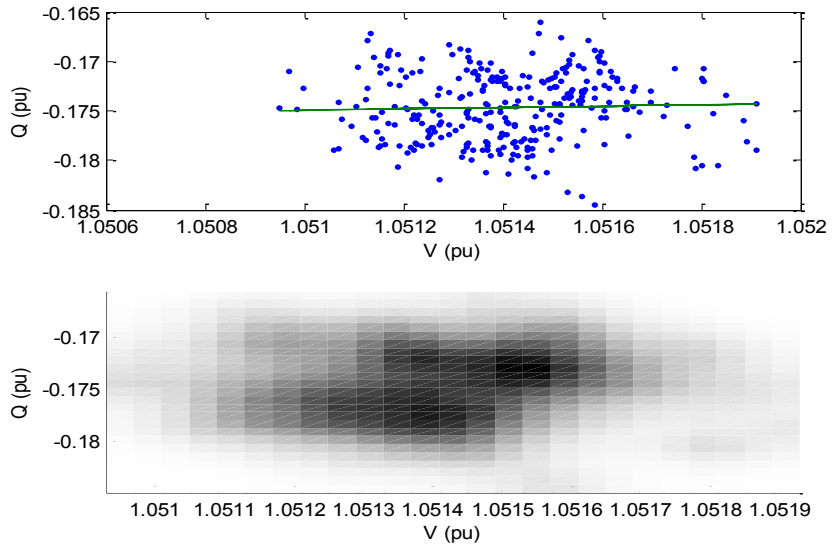

Figure 3.6 V-Q plot and the corresponding density plot in 10 seconds

This is typical. Usually, the graph of V vs. Q looks like disordered and even the linear fit method like Least-Square hardly tells the slope. Fig 3.6 is the collection of points during 10 seconds. We can see that the points distribute in a small area. There is no obvious trend for them. Their Least-Square fit line shows the slope is about 0.6509, which is not practical.

Still, we were attempting to show these points in their densities mode in order to observe how they behave in that area. But, there is no useful information, neither.

As mentioned before, the sign of the slope of the V vs. Q curve is always changing in the actual Synchrophasors not like SCADA data. Some factors can make trend positive and the others could make it negative. That is, the sign of slope is variable with regard to the time stamp. For the whole time period, plenty of positive and negative increments mix, which makes the whole trend look like flat. However, since the slope with only one positive sign or negative sign occurs at one moment or during one small piece time window, we are able to sort them in some way. Hence, Data Split has been designed.

Formally, Data Split is developed to separate the whole data points into two subsets: one with increasing trends (positive sensitivity) and the other with decreasing trends (negative sensitivity). This idea is simple but very useful. For the data set in Fig 3.6, we have two subsets shown in Fig 3.7 after data split.

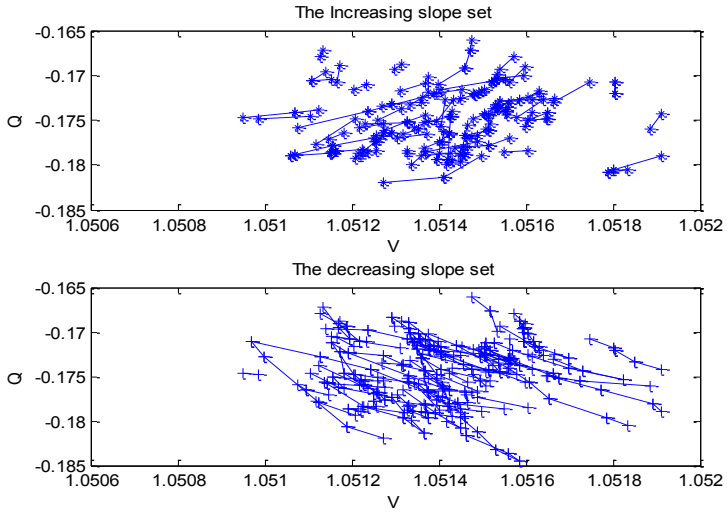

Figure 3.7 Two data subsets from Data Split

3.3.3 Weighted Average Slope

Not each slope in one subset can show the characteristics of the system at the time when it happens because of some casual or unknown disturbances. But numerous proper results tend to the real one or some reasonable region by the mean of statistics. Naturally, the mean value was considered first. However, this inevitably will lead to a dilemma. There is an obvious example: a data set contains ninety-nine 1 and one 100. The odd number 100 cannot reveal the true attribute but it pushes the mean value to be 1.99, which is almost twice of the true one. The same situation could be true when we handle the Synchrophasors. Although the very big variances, which are obviously wrong, have been deleted in Data Filter, some very small variances still remains. We do not want to discover if they are

wrong or not, or what cause them, we are paying attention to how to mitigate them. Similarly, one way to solve this problem is to introduce the slope thresholds: ΔQ_{err} and ΔV_{err}. When FBSC or BLA does the calculation, only the variances with $\Delta V_i > \Delta V_{err}$ or $\Delta Q_{ij} > \Delta Q_{err}$ or both can be taken into account for the slope calculation between two consecutive points. Here we use i and j to represent two ending buses of one transmission line for convenient purpose. For ending bus i, Q_{ij} is the line reactive power. The fact should be noticed in advance that the proposed FBSC utilizes ΔV_{err} and ΔQ_{err} simultaneously while BLA only use ΔV_{err} since no reactive flow occurs explicitly in this method. So, for a convenient way, only ΔV_{err} will be tuned for one special power system in that the slope is much more sensitive against change of bus voltage than line reactive power flow. The results from study is also support this decision. Again, tuning this threshold value is so sensitive that slight different values could give big different results. To demonstrate this fact, the following work has been done. Table 3.1 reveals the statistic estimations on three distinct Synchrophasors within 10 seconds, which will be used in the future in late this chapter. And, we will cite the results from the methods we did not introduce so far.

PMU	V_i (pu)		Q_{ij} (pu)	
Data	σ	μ	σ	μ
1	2.3023e-4	1.0517	0.006	-0.1749
2	2.76e-4	1.0443	0.0016	-0.1074
3	2.8384e-4	1.0245	0.007	-0.1724

Table 3.1 Statistical Estimation on Synchrophasors

As to Synchrophasor set 3, if $\Delta V_{err} = 1e-6$, the line sensitivities from two methods are approximately 56, -70 while they are about 38, -30 if $\Delta V_{err} = 1e-5$. By the reference from Jump, the latter approaches the meaningful one (42 only from Jump). Of course, Jump could give us a good way to tune this threshold. We have to be careful in tuning this threshold so that the correct or reasonable setting should make line sensitivity estimation close to the Jump value. The other way is trial and error. The good setting should make the results stable and consistent no matter which pieces of data are used, e.g. any 10 seconds data under no big event happens. The similar analysis will be done in this chapter as well.

On the other hand, the tuning process is trivial and the results are too sensitive against ΔV_{err} as we shown. Furthermore, the study on Synchrophasors often shows unstable results

though most of them are close to Jump value based on our experience. All of these encourage us to improve the approach. Hence Weighted Average Slope is proposed according to this demand.

For the data sets after Data Split, the Weighted Average Slope is defined as below:

$$\alpha(\beta) = \frac{(\sum_{i=1}^{n_1} X_{1i})n_1 + (\sum_{i=1}^{n_2} X_{2i})n_2 + \cdots \quad \sum_{i=1}^{n_k} X_{ki})n_k}{n_1 n_1 + n_2 n_2 + \cdots}$$

$$s.t.$$

$$X_{ki} \in \left((k-1)\bar{X} + a, k\bar{X} + a\right]$$

for increaing slope α, $\bar{X}$ is the length of interval and a is offset

$$or \qquad (3.1)$$

$$X_{ki} \in \left(-k\bar{Y} - b, -(k-1)\bar{Y} - b\right]$$

for decreaing slope β, $\bar{Y}$ is the length of interval and b is offset

Applying the case in the beginning of this section, the WAS (Weighted Average Slope) should be 1.01 that is really close to the true value. Here, we still need to set the proper values for $\bar{X}$, a and b. But, this work is not tough. Generally, a and b can simply be set to 0 unless there is a very special case when we do analysis on that. Simultaneously, $\bar{X}$ does not requirement so precise. Besides, the most important advantage is that using this method can relax the requirement on ΔV_{err}. This is a useful contribution since sometimes we do not have to worry about the threshold so much once we settle down one group of thresholds and even if there is some relatively big change. Let us see the results from the

same Synchrophasors (PMU #3) by using WAS method and the comparison between mean values and WASs. It is obvious that WAS is more stable and relaxes the constraint from the parameters.

Now, we have these effective ways to handle Synchrophasors and achieve the line sensitivities. For real time implementation, it is necessary to summarize a clear and practical approach. The next two sections will show the steps of FBSC and BLA respectively.

Setting	Sensitivity	0-10s	20-30s
$V_{err} = 1e-5$	α	37.06	34.36
Mean Value	β	-29.14	-39.48
$V_{err} = 1e-5$	α	37.06	33.14
WAS, $\bar{X}=300, \bar{Y}=100$	β	-24.35	-27.87
$V_{err} = 1e-6$	α	38.41	34.48
WAS, $\bar{X}=300, \bar{Y}=100$	β	-28.40	-29.71

Table 3.2 Sensitivities from FBSC by different setting

3.4 Fast Bidirectional Sensitivities Calculation (FBSC)

Each Synchrophasor data point provides bus voltage and its angle, the line current and its angle. The line reactive power Q_{ij} can easily be calculated (sometimes, Q_{ij} is directly known already from measurement equipments). Only using these pieces of information, FBSC can estimate the line sensitivity based on the following step:

a. *From Synchrophasors, calculate line reactive power Q_{ij} for each time stamp during some time period.*
b. *Form the data set $\{(V_i^k, Q_{ij}^k)\}$.*
c. *Filter the data set in terms of bad data and no measurements.*
d. *Calculate the slope for every two successive points in the data set.*
e. *By Data Split, two subsets are created.*
f. *Obtain the Weighted Average Slope for each subset as corresponding sensitivity.*

It is not hard to tell that the whole process of FBSC does not requirement the modal information of the power systems. Therefore, FBSC can be called "model-free" and will make the voltage stability assessment quite fast.

3.5 Bidirectional Linearization Approximation (BLA)

For practical applications, the back-up plan is always a good strategy because we can not only have the results for the more chances but also shoot trouble by comparing the results from both of them. Hence, another approach is developed to attain the line sensitivities by Synchrophasors partially.

Comparing the FBSC, BLA does not calculate line reactive power explicitly. As we know, the line reactive power can be expressed:

$$Q_{ij} = -V_i^2(B_{ij} + B_{i0}) - V_i V_j(G_{ij}\sin\delta_{ij} - B_{ij}\cos\delta_{ij}) \tag{3.2}$$

where B_{ij} and G_{ij} are the parameters of the line. B_{io} is the susceptance in the ending bus i. And $\delta_{ij} = \delta_i - \delta_j$. Essentially, Q_{ij} is the function of four variables: V_i, V_j, δ_i and δ_j. In the same way we introduced in Chapter 2, we have the following equations, some of which are identical to or similar with one of (2.3)—(2.5):

$$\frac{\partial Q_{ij}}{\partial V_i} = -2V_i(B_{ij} + B_{i0}) - V_j(G_{ij}\sin\delta_{ij} - B_{ij}\cos\delta_{ij}) \tag{3.3}$$

$$\frac{\partial Q_{ij}}{\partial V_j} = -V_i(G_{ij}\sin\delta_{ij} - B_{ij}\cos\delta_{ij}) \tag{3.4}$$

$$\frac{\partial Q_{ij}}{\partial \delta_i} = -V_i V_j(G_{ij}\cos\delta_{ij} + B_{ij}\sin\delta_{ij}) \tag{3.5}$$

$$\frac{\partial Q_{ij}}{\partial \delta_j} = V_i V_j(G_{ij}\cos\delta_{ij} + B_{ij}\sin\delta_{ij}) \tag{3.6}$$

$$\Delta Q_{ij} = \frac{\partial Q_{ij}}{\partial V_i}\Delta V_i + \frac{\partial Q_{ij}}{\partial V_j}\Delta V_j + \frac{\partial Q_{ij}}{\partial \delta_i}\Delta\delta_i + \frac{\partial Q_{ij}}{\partial \delta_j}\Delta\delta_j \tag{3.7}$$

But, the term $\frac{\partial Q_{ij}}{\partial \delta_i}\Delta\delta_i + \frac{\partial Q_{ij}}{\partial \delta_j}\Delta\delta_j$ will not affect so much since $\frac{\partial Q_{ij}}{\partial \delta_i} = -\frac{\partial Q_{ij}}{\partial \delta_j}$. Hence first-order partial equation should be:

$$\frac{\Delta Q_{ij}}{\Delta V_i} = \frac{\partial Q_{ij}}{\partial V_i} + \frac{\partial Q_{ij}}{\partial V_j}\frac{\Delta V_j}{\Delta V_i} \tag{3.8}$$

By (3.8), BLA directly obtains the slope between every two successive points. After Data Split and Weighted Average Slope, the two sensitivities are found. For another, BLA need more information beyond Synchrophasors: the line parameters. Fortunately, the line parameters are very stable for a long time. Below, we summarize this approach:

a. *The Synchrophasors from both endings of one line are used. But if there is no PMU in the other ending of the line, calculate* V_j *and* δ_j *via Synchrophasors in this ending and line parameters.*
b. *Form the data set* $\{(V_i^k, V_j^k)\}$.
c. *Filter the data set in terms of bad data and no measurements.*
d. *Calculate partial derivatives by line parameters by (3.3) and (3.4).*
e. *By (3.8), calculate the slope for every two successive points in the data set.*
f. *By Data Split, two subsets are created.*
g. *Obtain the Weighted Average Slope for each subset as the corresponding sensitivity.*

3.6 Jump

If the power systems were operating in normal conditions which mean no big events, then we can call the measurements from Synchrophasors to be ambient measurements. This name is also used in [20]. Then, if there is some event happening in the networks, the obvious changes must be captured by Synchrophasors so that the measurement data will show some extremely different shapes with ones only containing fluctuations. In fact, not

too big events but only ones like load increasing or capacitor/reactor switching can provide us a good opportunity to calculate the line sensitivities. Recall the method we used to make Q_i change in Chapter 2. Now we have the real time version. For vividly describing this big change, we define it as "Jump". Similar with the static method which is not affected by the dynamic response from the equipments in the power systems, Jump can make the results more accurate than the ones from fluctuations because of less dynamic factors. That is, we apply the points before and after the event to reveal the system's characteristics around operating point. But, we would not like to guarantee that Jump is absolutely accurate because we can not just ignore some dynamical attributes of the systems in such short time, like the exciters. For instance, there is always a "peak" occurring when the bus voltage changes a lot. It could result from the dynamical response of generators or just some devices' dynamical features.

On the other hand, by capturing the data in one certain time window before and after Jump, we calculate the line sensitivities. So this time window includes the "peak" time and the results from the Jump is sort of mixture of dynamic and static behaviors of the system. If we only consider the static response like power flow, no peak value occurs. The line sensitivity could be bigger. BUT, the calculation error may not be a significantly wrong when we assess the voltage stability by the global indices. We only care about the security

interval of the indices. Furthermore, if the load bus is far away from some big generators or the system experiences the voltage instability, the calculation errors among results are minor. The numerical cases will be given in the next sections.

Actually, the practical meaning of Jump or static approximation lies on helping us tune the parameters. Again, with respect to the model in Fig 3.1, Fig 3.8 shows one ideal relationship between fluctuation and Jump. Notice that the shapes of the solid lines are just for case, the real ones could be very different.

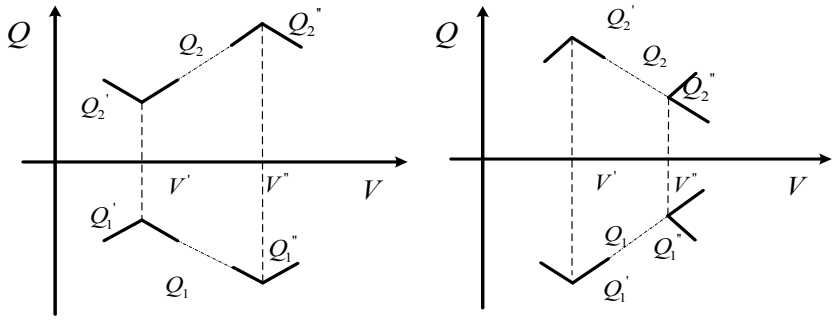

a b

Figure 3.8 The relationship between fluctuation and Jump

Here, $V^{'}$ and $V^{"}$ are the bus voltage before and after Jump. Then for Figure 3.8a and Fig 3.8b, we have (3.9) and (3.10) respectively.

$$\alpha_{Jump} = \frac{Q_2^{"} - Q_2^{'}}{V^{"} - V^{'}} \; in\,(a) \; or \; \frac{Q_1^{"} - Q_1^{'}}{V^{"} - V^{'}} \; in\,(b) \qquad (3.9)$$

$$\beta_{Jump} = \frac{Q_2^{"} - Q_2^{'}}{V^{"} - V^{'}} \; in\,(b) \; or \; \frac{Q_1^{"} - Q_1^{'}}{V^{"} - V^{'}} \; in\,(a) \qquad (3.10)$$

3.7 Tests on Simulation Systems

So far, the two proposed methods to calculate the line sensitivities by Synchrophasors have been introduced and explained in detail theoretically. Next, testing for them will be the crucial task to validate our designs. Although we have tons of real-time Synchrophasors from the practical power systems, like the Eastern Interconnection System in United States, it is better for demonstration to use some simulation systems because of their accessibility and repeatability. Moreover, they can be adjusted so that we can observe if the results from FBSC and BLA are equal or close to what it is expected.

Based on one classical and popular test system model: two-area system which can be found in [1] or the other literatures, one modified two-area system is shown in Fig 3.9.

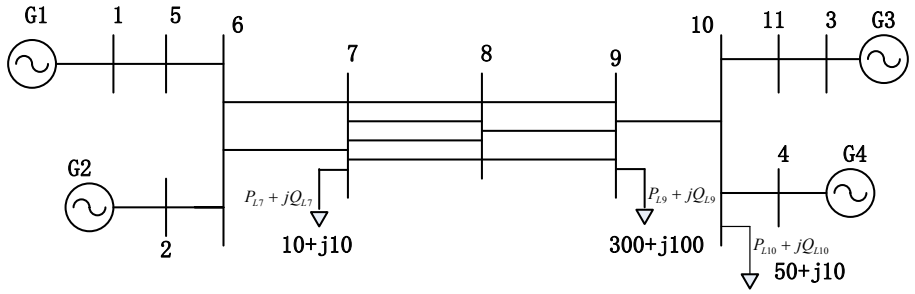

Figure 3.9 One modified two-area system

In order to make this test system more meaningful and practical like real system, some noise resources are imported to simulate the practical load fluctuation and noise. After importing of the noise resources, the statistic estimation of the data should be comparable with those in Table 3.1. Hence we did the several experiments as Table 3.3. In the viewpoint of the statistic estimation, scenario 2 and 3 can be candidates. In this dissertation, ***three noise sources with*** $\sigma = 1$ ***and*** $\mu = 0$ ***at bus 7, bus 9 and bus 8*** are chosen as the case.

1	One Noise Source with $\sigma = 1$ and $\mu = 0$ at bus 7			
	V_i		Q_{ij}	
	σ	μ	σ	μ
	1.0182e-4	1.0061	0.0024	-0.2876
2	Two Noise Sources with $\sigma = 1$ and $\mu = 0$ at bus 7 and bus 9			
	V_i		Q_{ij}	
	σ	μ	σ	μ
	4.1164e-4	1.0061	0.011	-0.2876
3	Three Noise Sources with $\sigma = 1$ and $\mu = 0$ at bus 7, bus 9 and bus 8			
	V_i		Q_{ij}	
	σ	μ	σ	μ
	4.2676e-4	1.0061	0.011	-0.2880
4	Three Noise Sources with $\sigma = 0.1$ and $\mu = 0$ at bus 7, bus 9 and bus 8			
	V_i		Q_{ij}	
	σ	μ	σ	μ
	4.1827e-5	1.0061	0.0011	-0.2878

Table 3.3 Statistical estimation on simulation data with noise

For another, for taking full advantage of the test system, we can build the similar systems with different security levels and the same noise sources so that we can verify the index Γ_i and line sensitivities simultaneously. There is an easy way which is to decrease the number of the generators. That is, use different numbers of generators to support the same load with the same topology. In other words, based on the described two-area system in Fig 3.9, the utilized testing systems are:

A. ***The two-area system with three 3 generators (G1, G2 and G3). Three noise sources with*** $\sigma = 1$ ***and*** $\mu = 0$ ***at bus 7, bus 9 and bus 8.***
B. ***The two-area system with only 2 generators (G1 and G2). Three noise sources with*** $\sigma = 1$ ***and*** $\mu = 0$ ***at bus 7, bus 9 and bus 8.***

For the sake of preciseness, the Table 3.4 reveals the statistic estimation on these test systems.

System	V_i		Q_{ij}	
	σ	μ	σ	μ
A	4.2676e-4	1.0061	0.011	-0.2880
B	0.0015	0.8089	1.6048e-4	0.0639

Table 3.4 Statistical estimation on two test systems

Although there are apparent differences, ΔV_{err} can be set to be same value, saying $1e-6$ if we apply Weighted Average Slope. Recall that WAS method will relax the requirement from the threshold.

System B is modified from System A. Generator 3 is off service and the big amount of shunt capacitors is added in Bus 8 in order to keep the bus voltage in reasonable region. Although the voltages at Bus 9 in two systems are similar, they are having extremely different security level. For System B from Table 3.5, the index is lower than 10, which means that the current operation is close to collapse. The same illustration can be found in the graph. If the two lines of three parallel tie lines between Bus 8 and Bus 9 are of outage at 15 seconds, the System B collapses (very low bus voltage is not real in real power system). On the other hand, System A is strong enough even though it experiences the same contingency. The responses are shown in Fig 3.10.

Test Systems	A					B				
	9-10		**9-8**		Γ_9	**9-10**		**9-8**		Γ_9
	α	β	α	β		α	β	α	β	
FBSC	**10**	-14	**3**	-5	**19**	**1.5**	-0.1	**1.7**	-3.6	**6.6**
BLA	**11**	-16.4	**2.4**	-3.2	**18.2**	**1.8**	-0.21	**1.7**	-2.4	**6.9**
Jump	**17**	-12	**3.2**	-6	**26.6**	**0.15**	-10	**3.3**	-0.5	**10.05**

Table 3.5 Line sensitivity estimations and the indices

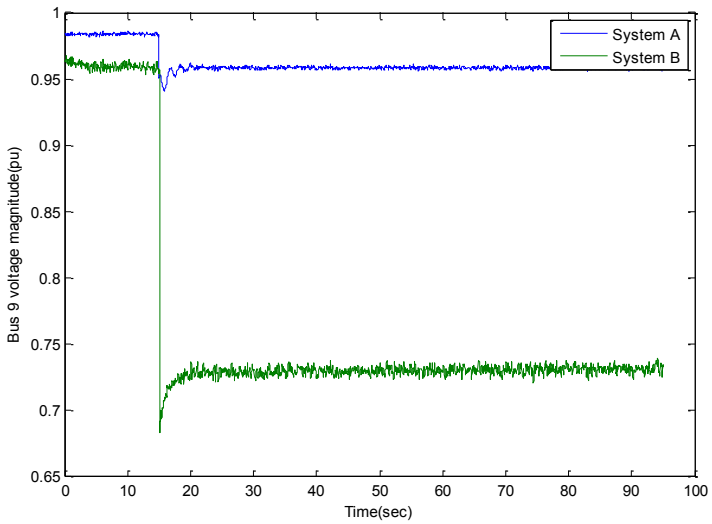

Figure 3.10 Bus voltage responses after tripping of double lines

3.8 Tests on Real Synchrophasors

First all, all Synchrophasor data we used in the dissertation are measured from real systems. They came from the Eastern System or Western System in United States. But, for the confidential purposes, their names, locations and the exact time will be deleted. We only describe the data in per unit format, such as bus voltage and line reactive power flow. The base KV will not be specified but base power is 100MVAR as normal so that readers can understand the meaning of the sensitivity better.

FBSC will be tested for each set of Synchrophasors since it only requires least information. If there is PMU in the other ending bus of the line or we can access the parameters of that line, BLA is also tested in order that the results from both algorithms can be compared. Moreover, once some Jump occurs during that period, the sensitivity from that Jump is represented.

Theoretically, we could use any data with any length of time window set to calculate line sensitivity, but in a meaningful and practical way we will choose 1-second and 10-seconds data in this paper in order that we can show the influence of the different lengths of time windows on the estimations. And the statistic estimations of the data for three PMUs have been shown in Table 3.1. Simply, for all cases, $\Delta V_{err} = 1e-6$. After tuning and for better results on that PMU, $(50,50)$ are set for both Test A and Test B and $(300,100)$ is with

Test C for the increasing interval and decreasing interval respectively used by WAS method.

3.8.1 Test on PMU #1

This test is a "one-way" test since we have no way to access the transmission line parameters. So only FBSC is be used. Fig 3.11 is the snapshot of the 200-seconds data. There are two Jumps occurring around 760 second and 840 second. Fig 3.12 is about two subsets around 760 second after Data Split. The obvious distance can be easily found.

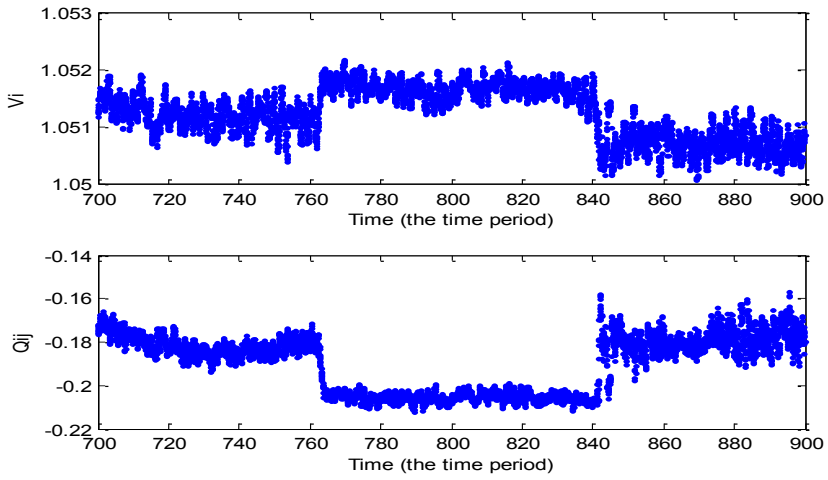

Figure 3.11 V-Time and Q-Time from 700s to 900s data

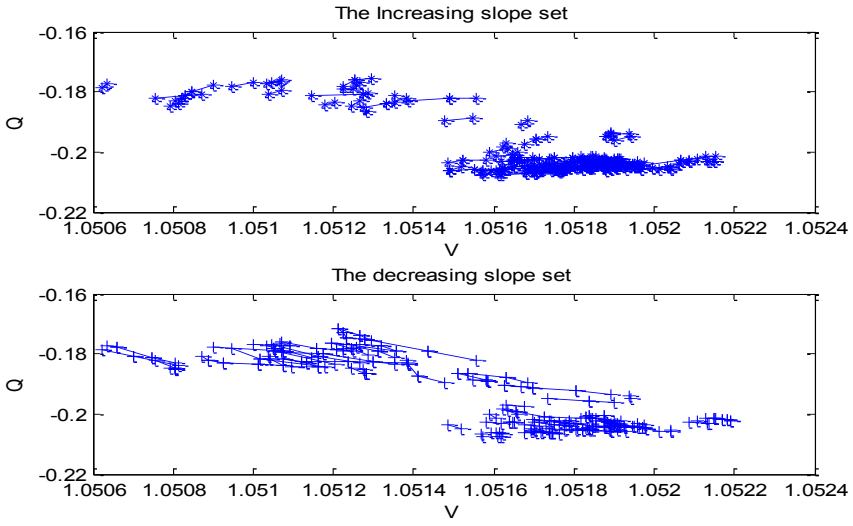

Figure 3.12 V-Q pairs for 10-second from after Data Split

Table 3.6 shows the results from FBSC and Jump. We can see they are well comparable. And the event slightly affects the negative line sensitivities and they came back after event. In addition, this is a real example of the case in Fig 3.8b.

Sensitivity	700s-701s	700s-710s	800s-801s	800s-810s	860s-861s	860s-870s
α	22.73	19.61	16.50	17.45	17.15	21.82
β	-28.49	-21.88	-13.01	-15.63	-24.52	-22.82
β_{Jump}	-24.4831 around 760s and -26.2965 around 840s					

Table 3.6 Sensitivities from FBSC on PMU #1

3.8.2 Test on PMU #2

These Synchrophasors were captured when the system experienced some test events. That is, we know the system was injected by some sorts of noise. The magnitude could be ± 5 MW or ± 10 MW at different nodes. Since we have the network parameters for this system, FBSC and BLA can be used simultaneously. The snapshot of the first 200-second data is shown in Fig 3.13. Apparently, there is a period when no measurement happened (maybe circuit break was open).

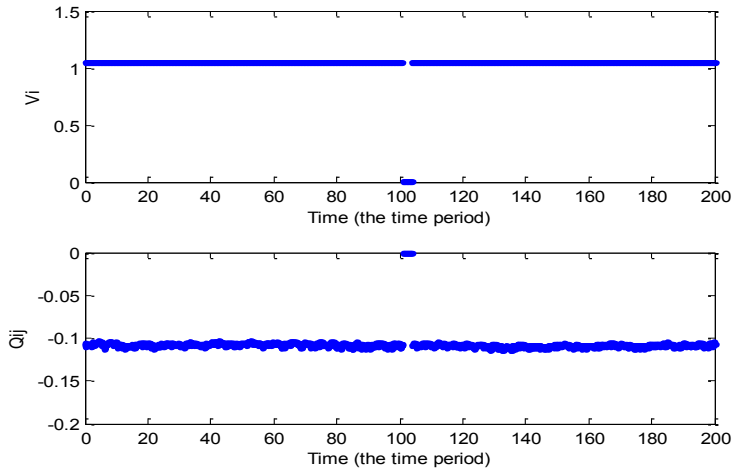

Figure 3.13 V-Time and Q-Time from 0s to 200s data

The first 10-second data and its subsets are shown in Fig 3.14 and 3.15. And the line sensitivities are in Table 3.7 and Table 3.8.

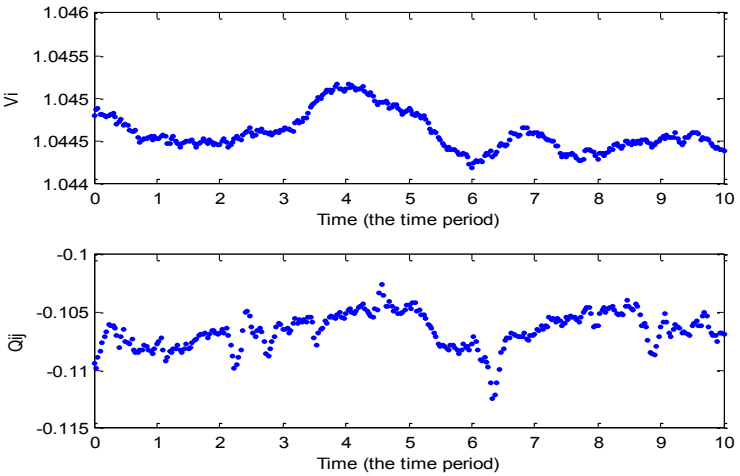

Figure 3.14 V-Time and Q-Time for first 10-second data

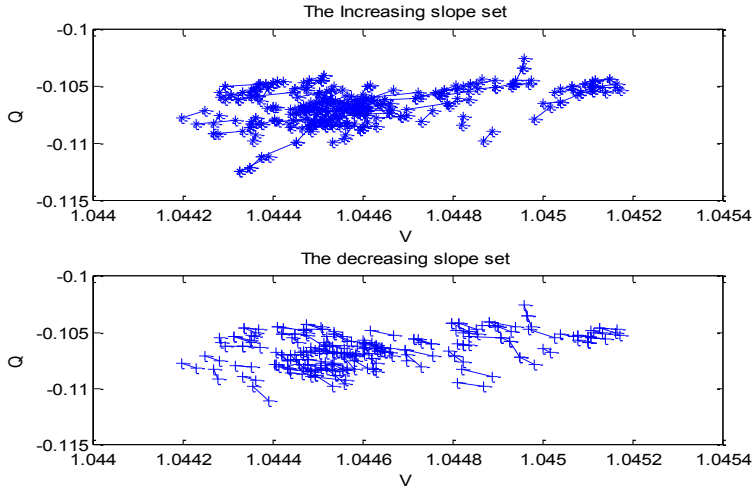

Figure 3.15 V-Q pairs for first 10-second data from Data Split

Sensitivity	0s-1s	0s-10s	50s-51s	50s-60s	150s-151s	150s-160s
α	16.64	14.77	10.13	15.21	17.87	15.79
β	-18.73	-14.81	-12.85	-15.43	-16.57	-13.25

Table 3.7 Sensitivities from FBSC on PMU #2

Sensitivity	0s-1s	0s-10s	50s-51s	50s-60s	150s-151s	150s-160s
α	21.76	15.86	10.97	16.54	20.78	17.32
β	-20.97	-15.51	-14.26	-18.43	-22.32	-15.60

Table 3.8 Sensitivities from BLA on PMU #2

3.8.3 Test on PMU #3

This test is with Jump around 35 second like Fig 3.16 showing. Fig 3.17 is the subsets between 30s-40s.

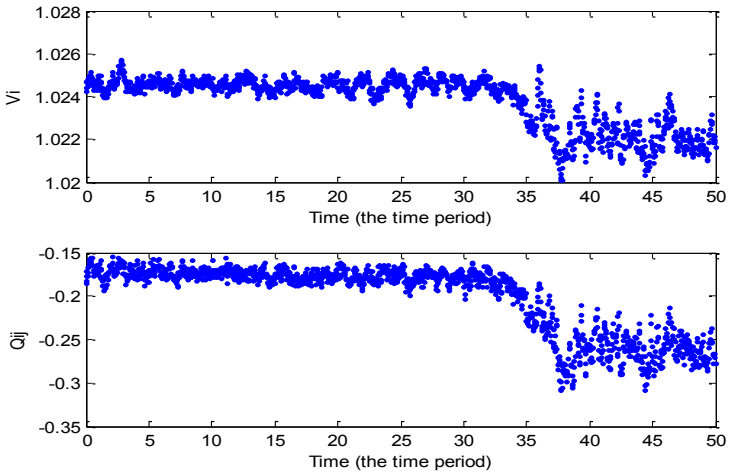

Figure 3.16 V-Time and Q-Time from 0s to 50s data

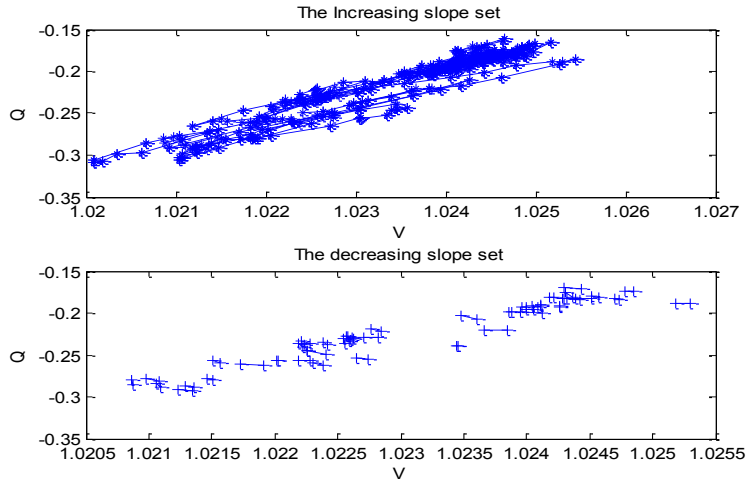

Figure 3.17 V-Q pairs for 30s-40s data from Data Split

Sensitivity	0s-1s	0s-10s	30s-31s	30s-40s	40s-41s	40s-50s
α	38.66	38.41	49.51	41.29	28.91	36.11
β	-22.42	-28.40	-42.01	-30.36	-27.88	-40.67
α_{Jump}	42.33 around 35s					

Table 3.9 Sensitivities from FBSC on PMU #3

Sensitivity	0s-1s	0s-10s	30s-31s	30s-40s	40s-41s	40s-50s
α	39.50	38.54	47.46	38.60	27.73	34.77
β	-18.04	-22.07	-41.10	-29.23	-23.77	-41.23

Table 3.10 Sensitivities from BLA on PMU #3

Again, the estimated line sensitivities from either FBSC or BLA in Table 3.9 and 3.10 are confident.

3.9 Real-time Monitoring Case from a Real Power System Implementation

Instead of showing line sensitivities in the tables, the proposed global voltage stability assessment index can be demonstrated below because we can access all line information

for some buses which are in this system and which have PMU installation. This on-line monitoring prototype works with openPDC (previously superPDC) so that the detecting is in real-time. The output of the monitoring will be archived into one SQL database and the alarm will be trigged once some low indices are found. Also, some parameters can be chosen and tuned for different PMU settings or PMU equipments.

Fig 3.18 illustrates a snapshot of on-line monitoring process around one minute. The indices are chosen from 3 PMUs: PMU1-500KV, PMU2-500KV&161KV and PMU3-161KV. As we know, in normal operation condition, one 500KV bus should be ”stronger” than the lower KV buses except that only few transmission lines are connected with this 500KV bus.

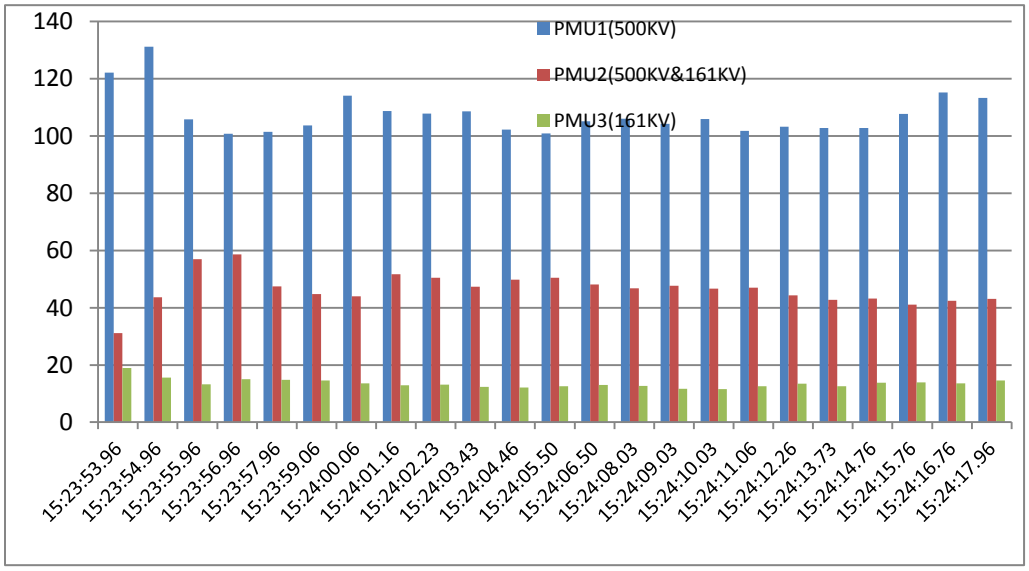

Figure 3.18 The global VSA indices from three buses in real time

3.10 Summary

This chapter discussed two methodologies in which the line sensitivity φ_i can be estimated only or partly by Synchrophasors. So, first the theoretical analysis demonstrated the rationalities of the existing of the positive and negative slopes in power systems. Then we analyzed the actual Synchrophasors in detail. Although the fluctuation, which is the most common format of Synchrophasors normally during some time interval, looks like disordered and useless, it does contain the variances with the positive or negative slopes. Therefore, Data Split was developed to deal with the fluctuation in order to separate the whole data set into two subsets, one of which has the positive slopes and the other has the negatives. For each subset, instead of simple computing mean value, Weighted Average Slope is designed to obtain more stable and consistent estimations and in the same time to relax the requirement from the threshold because we have consider the influence of the statistic characteristics of the Synchrophasors. For another, the further consideration is about the relatively big change in Synchrophasors, which maybe comes from certain event. Such much clearer and distinctive shape in Synchrophasors can give us a good reference to verify the results from the fluctuations.

The tests done for validating our designs in this chapter are also comprehensive. Those two simulation systems based on two-area test system are very good cases proving the

validations of FBSC and BLA. Even the conclusion on the voltage stability assessment index is also verified very well. Frankly speaking, it is hard to know all information to compare the estimation we made from actual Synchrophasors. However, those three tests on actual Synchrophasors have accomplished this mission. Processing the randomly chosen data set, FBSC and BLA give the stable and consistent estimations already. And some of them have been referred by Jumps. Therefore, these results are meaningful and useful. In other words, these two methodologies are of feasibility.

A prototype of on-line monitoring tool has been developed to work with openPDC in a utility so that the real-time, fast, accurate and reasonable voltage stability assessment is feasible now.

In the next chapter, another application of the line sensitivities and the VSA indices will be introduced: real-time voltage control.

Chapter 4

Real Time Voltage Control:

Advanced Local Voltage Controller

The previous chapters have developed the approaches to assess the current voltage stability in only few seconds by Synchrophasors. For one thing, this voltage stability assessment could make it possible that the voltage controllers quickly response to the voltage problem. For another, the VSA index and the line sensitivity already carry the system information coming from Synchrophasors. The controller should be able to utilize these pieces of information to improve the performance of the control actions, such as predictability, accuracy and rapidity.

This chapter proposes an Advanced Local Voltage Controller to fulfill this task. In our normal consideration, this controller has two parallel control structures as well: model-free and model-based. Based on the each individual framework, the corresponding local voltage predictor is used to estimate the control effects after some control device is chosen based on the resource of the information: Synchrophasors and Synchrophasors/SCADA

respectively. The crosscheck is designed simultaneously so that the large difference between them can be found. Moreover, the control action is of optimization because some practical and feasible objective function is utilized to select the final decision among many choices.

4.1 Real-time Voltage Control Framework

The main task of real-time voltage control is to automatically perform a control action or trigger an alarm to system operators in substation level in terms of the current local system states. All common reactive compensation devices such as the shunt capacitors/reactors and SVCs and the other voltage regulation devices such as LTCs should be included in the regulated objectives. Meanwhile, considering some certainly practical control rules obeyed by the experienced system operators such as the order in which the devices will be switched, the minimum switching and the maximum available control devices, the controller should do the same things and even more. Based on the above ideas, the real-time voltage control framework is shown in Fig 4.1.

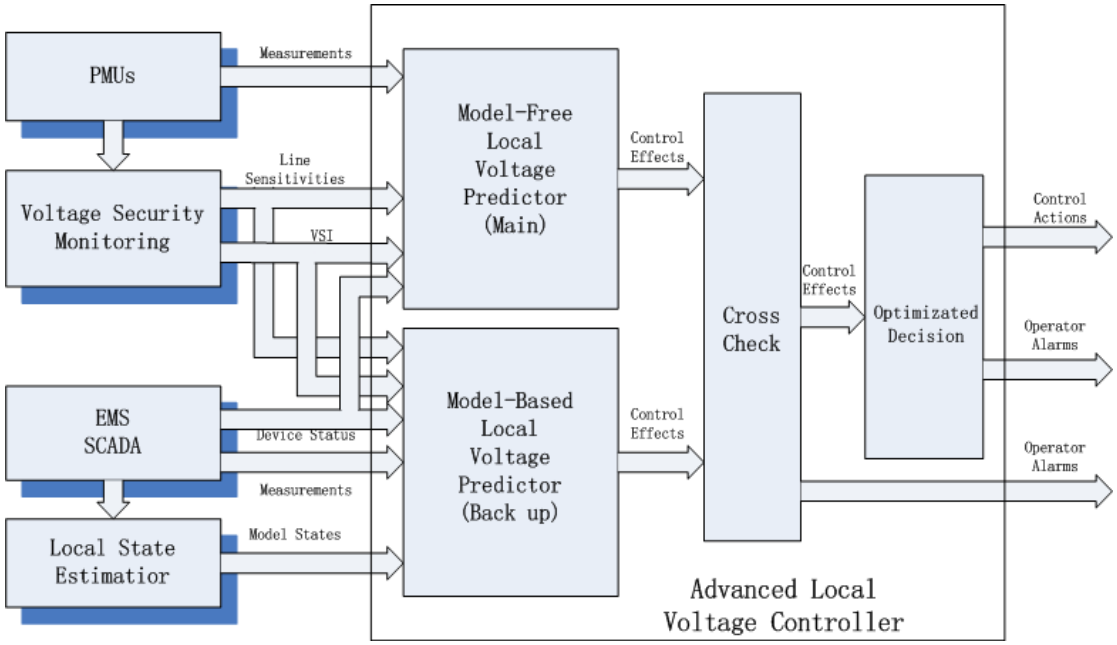

Figure 4.1 Real-time voltage control framework

The Synchrophasors will be the main data source. The Advanced Local Voltage Controller will use the global VSA indices coming from the designed monitoring tool indirectly to determine if the control action or the alarm is needed. For another, it will predict influence the control action by synthesizing Synchrophasors and the results from the real-time voltage monitoring part as well. This process does not require any information from system models. On the other hand, SCADA/SE can be the back-up data source. There is another predictor with totally different structure as the back-up in the Advanced Local Voltage Controller. This back-up predictor can accept either

Synchrophasors or SCADA data but it does need the system branch parameters to predict the control action so the SE becomes required.

The Local Voltage Predictor (LVP) is designed to estimate the voltage change after some control device is switched which is supposed to be used. The main predictor completes this procedure only via information directly and indirectly from PMUs so that it does not do any power flow calculation. To the contrary, the back-up predictor will use least-square method to solve one group of linear equations which are linearized power flow equations in some sense to predict the voltage increments. In normal conditions, the results from two predictors should have no significant differences and then all the control effects will be sent to the optimization block and the final control decision will be made. But, if there is something wrong such as topology errors or significant measurement errors, the obviously distinct predictions will be observed. At this time, one alarm will be triggered in order to inform the system operators who can figure out which part is in trouble and decide which control action is able to be performed.

In summary, the following flowchart shows the whole control procedure of the Advanced Local Voltage Controller from receiving the measurements to sending a control action.

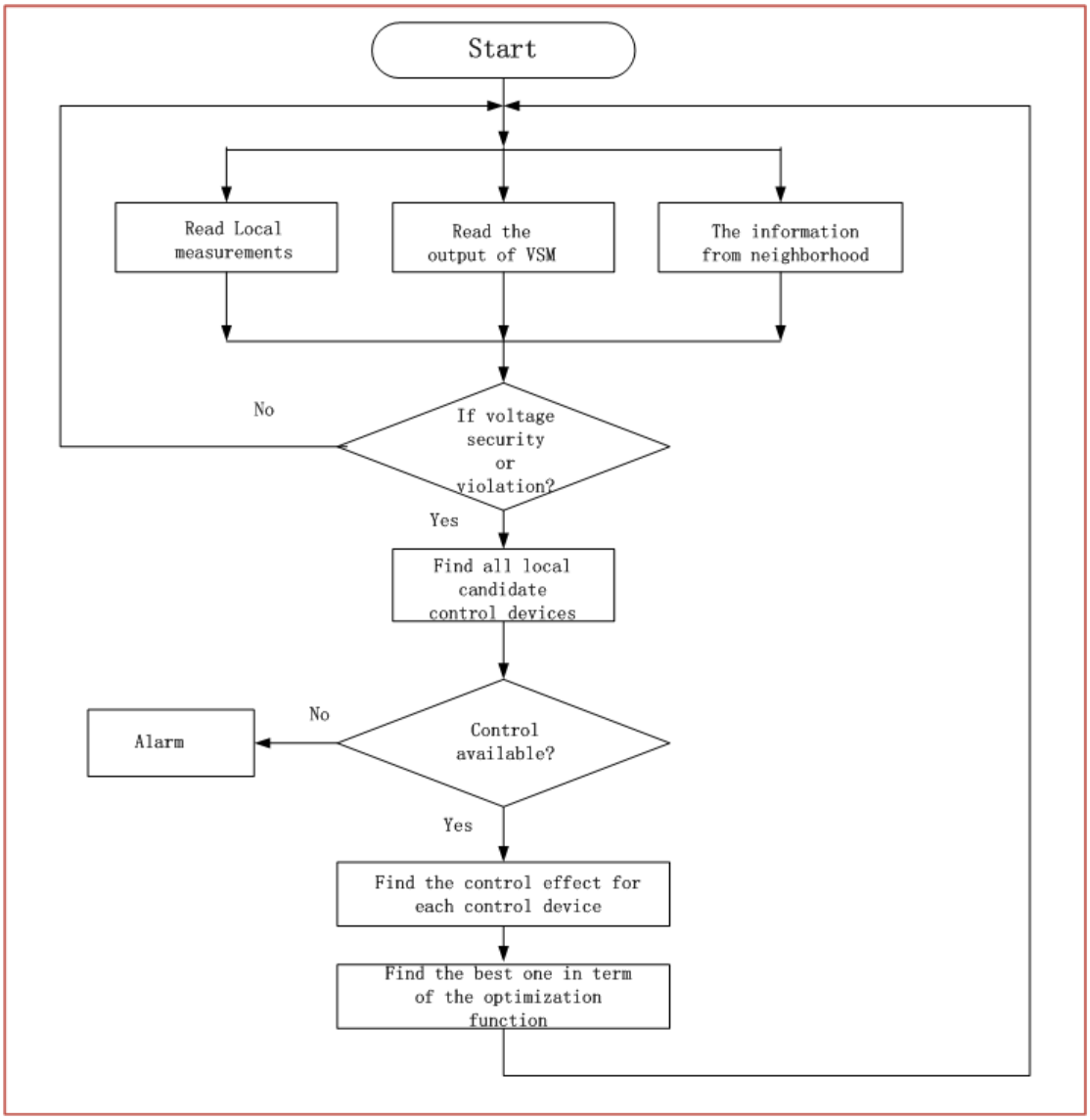

Figure 4.2 Advanced Local Voltage Controller flowchart

The Advanced Local Voltage Controller reads the measurements from Synchrophasors and SCADA/SE. In the same time, the information from the voltage monitoring part is accepted to determine if the current buses are experiencing or potentially facing some

voltage problems which mean that certain control actions are necessary. The next stage is to predict the control effects by LVP for all available control devices in the local area. Of course, sometimes if all control devices are running out, an alarm is sent to the system operators. The last stage is to choose the "best" one among all available control devices. This is an optimization process. That is, this "best" choice is able to satisfy a few optimal requirements, such as the minimization of switching cost and the maximization of reactive compensation reserve. Once one "best" control device has been picked up, the corresponding control action will be performed. And then this entire procedure will be gone through again.

4.2 Local Voltage Predictor

The Local Voltage Predictor is proposed to calculate the voltage changes at the buses after one voltage control device is assumed to be used. Traditionally, the full power flow calculation will achieve each bus voltage change perfectly when some device status changes. But, considering the application of the local voltage control, only local power subsystem will be taken account into. Hence, calculating the full power flow will be time-consuming and unnecessary. Further, accessing the full system information is not practical in substation level. On the other hand, each of buses in one entire power system has PMU installation is not realistic in the current circumstance but this fact is easily to be

realized in some small areas or some neighbouring substations. Based on these local measurements, the local voltage controller should be able to predict the local bus voltage changes which are accurate enough and closed to those resulting from full power flow calculation.

As to the control devices, all the available shunt reactive power compensation devices and LTC transformers for some certain scenarios will be considered as candidates. For example, for low voltage violation, the shunt capacitors which are open currently, the shunt reactors which are now close, the SVCs and LTCs which are not reaching limits will be considered as the candidates. The predictors will evaluate the influence from the switching of each device and tap changing among these candidates. But, there is one basic distinction between both predictors. The model-free LVP is voltage-based. That is, it treats the control devices as the continuous ones because it will get the requested voltage deviation first and then find the closest amount or tap. To contrast, the model-based LVP thinks of the control devices as the discrete ones. It first assumes certain amount change or some tap changes and then calculates the voltage variances. If those voltages after controls would eliminate or mitigate the voltage violation and improve the voltage profiles, the assumed amounts or tap changes will be selected. Otherwise, the searching process will continue until the final results are found or all devices are run out.

4.2.1 Model-free Local Voltage Predictor

1. Formulation

Like Phasor Data Concentrator (PDC), if the PMUs can share their information among the substations in the local system, the voltage forecasting will become easier. That is, the local voltage controller should collect the Synchrophasors in its local control area. Other than the only one certain bus, any bus voltage change is able to be forecasted when any control action is done anywhere in this local system. This process does not request the local system model. Essentially, Synchrophasors are sufficient. But, of course, the additional information from the designed voltage monitoring tool in the previous chapter is also needed to accomplish this mission. The Fig 4.3 shows the case of the form of information sharing between two PMUs in the two endings of one branch.

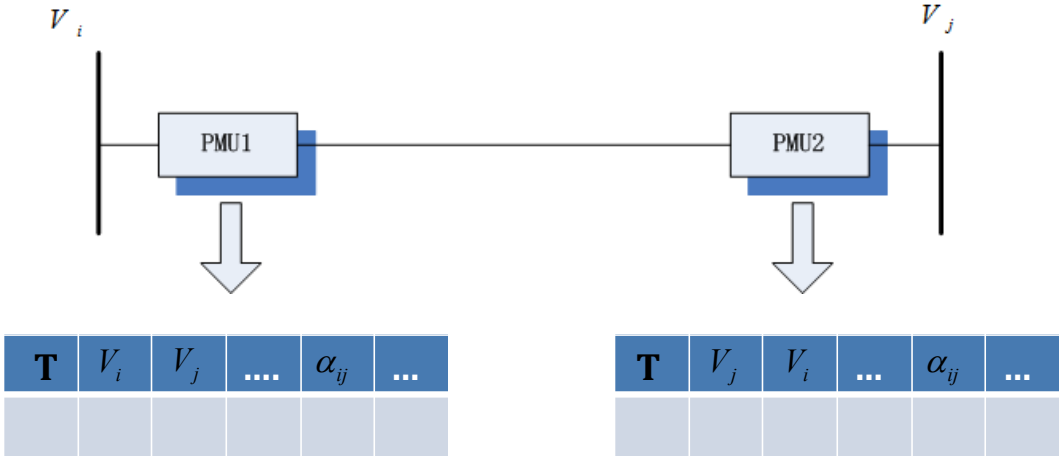

Figure 4.3 Form of information sharing between PMUs

Suppose the voltage violation or the potential voltage stability problem occurs in bus i, the controller will consider the available control devices at bus i first and the nearest and available ones centered by bus i, which is obeying the voltage control characteristics. This process is related to the priority issue associated with optimization selection. Here, the only concern is the location of the control devices.

i). If the control devices are at bus i, and then the controller can predict how much reactive power compensation is demanded and what the voltage at bus j will be. Fig 4.4 easily summarizes this process.

$$\Delta V_i \xrightarrow{\Gamma_i} \Delta Q_i \xrightarrow{\alpha_{ij}} \Delta Q_{ij} \xrightarrow{\approx} \Delta Q_{ji} \xrightarrow{\beta_{ji}} \Delta V_j$$

Figure 4.4 The process of prediction for control devices at bus i

For the requested voltage change to delete or mitigate the violation or potential stability problem, the VSA index Γ_i is the shortcut for calculating the requested amount the reactive power compensation. Meanwhile, according to the definition in Chapter 3, the line sensitivities α_{ij} and β_{ji} can make the controller know the effect on the voltage at bus j.

ii). Similarly, if the control devices come from bus j, the controller has to know how the control action can relieve the voltage violation or stability problem at bus i. In this time, ΔQ_j or ΔV_j will happen first and ΔV_i follows as shown in Fig 4.5.

$$\Delta Q_j \xrightarrow{\Gamma_j} \Delta V_j \xrightarrow{\alpha_{ji}} \Delta Q_{ji} \xrightarrow{\approx} \Delta Q_{ij} \xrightarrow{\beta_{ij}} \Delta V_i$$

Figure 4.5 The process of prediction for control devices at bus j

2. Example

By the previous results from the test systems used in this thesis, the effective performance can easily be committed.

Recall the 9-bus case in Chapter 2. As to the example that i is Bus 9 and j is Bus 8, the following values from the calculation:

	Γ	α	β
Bus 9	$\Gamma_9 = 10.64$	$\alpha_{98} = 4.06$	$\beta_{98} = -5.946$
Bus 8	$\Gamma_8 = 22.406$	$\alpha_{89} = 2.643$	$\beta_{89} = -18.577$

Table 4.1 VSI and line sensitivities for Bus 8 and Bus 9 of 9-bus system

the Γ_9 is 10.64. And there are two lines connected with Bus 9, which have line sensitivities 4.058(α_{98}) and 6.581(α_{94}). Thus, if the voltage in Bus 9 has 0.01 p.u. increase through 10.64 Mvar compensation at Bus 9 calculated by $0.01 \xrightarrow{*10.64} 0.1064$, the Bus 8 will have voltage increase 0.007 p.u. calculated by $0.01 \xrightarrow{*4.058} 0.04058 \xrightarrow{/18.577} 0.002$.

In fact, if we add 10.64 Mvar compensation at Bus 9 and run Power Flow, we will have Bus 9 voltage change from 0.958 p.u. to 0.967 p.u. and Bus 8 voltage change from 0.9962 p.u. to 0.9985 p.u. . The error percentage is only 0.1% and 0.05%, respectively.

On the other hand, assume there are 20 Mvar capacitor added at Bus 8, by the formulation in (ii), Bus 8 will have voltage increase by 0.0089 p.u. and Bus 9 does 0.004 p.u. . By the Power Flow calculation, the voltage on Bus 8 changes from 0.9962p.u. to

1.0052 p.u. while that on Bus 9 changes from 0.958 p.u. to 0.9624 p.u. . This time, the estimation error percentages are less than 0.01%

4.2.2 Model-based Local Voltage Predictor

Here, we have to separate the formulations into two major aspects since the control devices are thought as having discrete behaviors. In the beginning, the (2.2) is still one basis which is renumbered in this chapter and additionally the bus current I_i is another.

$$Q_{ij} = -V_i^2(B_{ij} + B_{i0}) - V_i V_j(G_{ij}\sin\delta_{ij} - B_{ij}\cos\delta_{ij}) \tag{4.1}$$

$$\vec{I}_i - \sum_j \vec{I}_{ij} + \sum_j \vec{I}_{ij0} + \sum_L \vec{I}_i + \sum_S \vec{I}_i = 0 \tag{4.2}$$

In (4.2), the first item represents branch current by the branch admittance. The second item is for shunt admittance of that branch. The third comes from load and the last one is showing current in shunt devices.

1. Shunt Reactive Power Compensation Devices

Expanding the equations (4.1) by Taylor's equation, we have:

$$\begin{aligned} &\Delta Q_{ij} = \Delta Q_{ij}(\Delta V_i, \Delta V_j) = \frac{\partial Q_{ij}}{\partial V_i}\Delta V_i + \frac{\partial Q_{ij}}{\partial V_j}\Delta V_j + O(V_i, V_j) \\ &\Rightarrow \Delta Q_i = \sum_j \left[\frac{\partial Q_{ij}}{\partial V_i}\Delta V_i + \frac{\partial Q_{ij}}{\partial V_j}\Delta V_j \right] \end{aligned} \tag{4.3}$$

And the detailed version of (4.2) is shown as (4.4).

$$\sum_j [(V_i \angle \delta_i - V_j \angle \delta_j)(G_{ij} + jB_{ij})] + V_i \angle \delta_i \sum_j (G_{ij0} + jB_{ij0}) + \left[\frac{-jQ_s}{V_i \angle \delta_i}\right]^* + \left[\frac{P_i + jQ_i}{V_i \angle \delta_i}\right]^* = 0 \tag{4.4}$$

Where Q_s is the shunt reactive power compensation devices and the load demand is P_i and Q_i. The others have the same definitions as those in Chapter 2. Based on the Kirchhoff's Laws, the new I_i should be equal to zero as well after the shunt device is added at the bus. Assuming the bus angles are constant with respect to the voltage issues, the new I_i can be rewritten to (4.5):

$$\sum_j \{[(V_i + \Delta V_i) \angle \delta_i - (V_j + \Delta V_j) \angle \delta_j](G_{ij} + jB_{ij})\} + (V_i + \Delta V_i) \angle \delta_i \sum_j (G_{ij0} + jB_{ij0}) + \left[\frac{-j(Q_s + \Delta Q_s)}{(V_i + \Delta V_i) \angle \delta_i}\right]^* + \left[\frac{P_i + jQ_i}{(V_i + \Delta V_i) \angle \delta_i}\right]^* = 0 \tag{4.5}$$

In order to make (4.5) linear with respect to ΔV_i, we consolidate the last two terms of (4.5):

$$\left[\frac{-j(Q_s + \Delta Q_s)}{(V_i + \Delta V_i) \angle \delta_i}\right]^* + \left[\frac{P_i + jQ_i}{(V_i + \Delta V_i) \angle \delta_i}\right]^* = \left[\frac{P_i + j(Q_i - Q_s - \Delta Q_s)}{(V_i + \Delta V_i) \angle \delta_i}\right]^* = \frac{1}{V_i + \Delta V_i}\left[\frac{P_i + j(Q_i - Q_s - \Delta Q_s)}{\angle \delta_i}\right]^*$$

Since $\frac{1}{V_i + \Delta V_i} = \frac{1}{V_i} - \frac{\Delta V_i}{V_i^2} + O(\Delta V_i)$, (4.5) will have another induced equivalence:

$$\sum_j \{[(V_i + \Delta V_i)\angle\delta_i - (V_j + \Delta V_j)\angle\delta_j](G_{ij} + jB_{ij})\} + (V_i + \Delta V_i)\angle\delta_i \sum_j (G_{ij0} + jB_{ij0})$$
$$+(\frac{1}{V_i} - \frac{\Delta V_i}{V_i^2})\left[\frac{P_i + j(Q_i - Q_s - \Delta Q_s)}{\angle\delta_i}\right]^* = 0 \quad (4.6)$$

Apparently, the equation (4.6) will introduce two equations: real and image parts of the currents for bus i. For the sake of simplicity, (4.3) and (4.6) will be re-expressed by the new and simple symbols as:

$$\Delta Q_i = \Delta V_i \sum_j^{n_j} a_{ij} + \Delta V_1 b_{i1} + ... + b_{in_j} \Delta V_{n_j} \quad (4.7)$$

$$-[\sum_j^{n_j} (h_{ij} + k_{ij}) + g_i] = \Delta V_i [\sum_j^{n_j} (c_{ij} + e_{ij}) + f_i] - \Delta V_1 d_{i1} - ... - \Delta V_{n_j} d_{in_j} \quad (4.8)$$

$$-[\sum_j^{n_j} (\bar{h}_{ij} + \bar{k}_{ij}) + \bar{g}_{ij}] = \Delta V_i [\sum_j^{n_j} (\bar{c}_{ij} + \bar{e}_{ij}) + \bar{f}_i] - \Delta V_1 \bar{d}_{i1} - ... - \Delta V_{n_j} \bar{d}_{in_j} \quad (4.9)$$

Here,

$a_{ij} = -2V_i(B_{ij} + B_{ij0}) - V_j(G_{ij}\sin\delta_{ij} - B_{ij}\cos\delta_{ij})$,

$b_{ij} = -V_i(G_{ij}\sin\delta_{ij} - B_{ij}\cos\delta_{ij})$,

$c_{ij} = \cos\delta_i G_{ij} - \sin\delta_i B_{ij}$,

$d_{ij} = \cos\delta_j G_{ij} - \sin\delta_j B_{ij}$,

$$e_{ij} = \cos\delta_i G_{ij0} - \sin\delta_i B_{ij0},$$

$$f_i = -\frac{P_i \cos\delta_i + (Q_i - Q_s - \Delta Q_s)\sin\delta_i}{V_i^2},$$

$$g_{ij} = \frac{P_i \cos\delta_i + (Q_i - Q_s - \Delta Q_s)\sin\delta_i}{V_i},$$

$$h_{ij} = G_{ij}(V_i \cos\delta_i - V_j \cos\delta_j) - B_{ij}(V_i \sin\delta_i - V_j \sin\delta_j),$$

$$k_{ij} = V_i(\cos\delta_i G_{ij0} - \sin\delta_i B_{ij0}),$$

$$\bar{c}_{ij} = \sin\delta_i G_{ij} + \cos\delta_i B_{ij},$$

$$\bar{d}_{ij} = \sin\delta_j G_{ij} + \cos\delta_j B_{ij},$$

$$\bar{e}_{ij} = \sin\delta_i G_{ij0} + \cos\delta_i B_{ij0},$$

$$\bar{f}_i = -\frac{P_i \sin\delta_i - (Q_i - Q_s - \Delta Q_s)\cos\delta_i}{V_i^2},$$

$$\bar{g}_{ij} = \frac{P_i \sin\delta_i - (Q_i - Q_s - \Delta Q_s)\cos\delta_i}{V_i},$$

$$\bar{h}_{ij} = B_{ij}(V_i \cos\delta_i - V_j \cos\delta_j) + G_{ij}(V_i \sin\delta_i - V_j \sin\delta_j),$$

$$\bar{k}_{ij} = V_i(\cos\delta_i B_{ij0} + \sin\delta_i G_{ij0}).$$

The subscript i means the center bus in this local control area, which has the certain shunt device Q_s. Meanwhile, j represents those PQ buses that directly connect to this center bus and n_i is the total number of such buses.

2. Load Tap Changers

Although there is no reactive power compensation at buses when transformers change their taps, the topology parameters will be changed. Consider the LTC model shown in Fig 4.6.

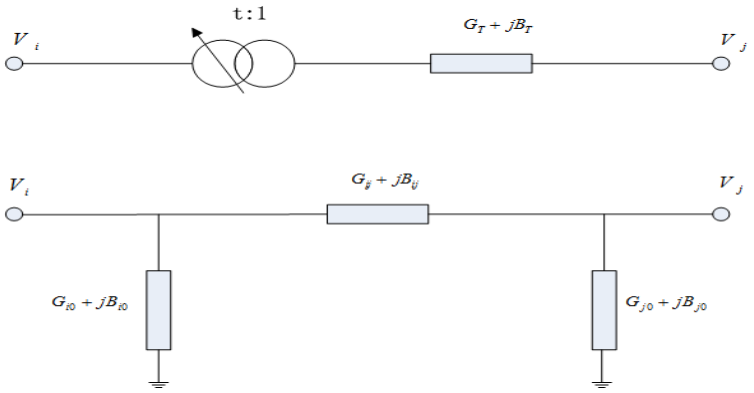

Figure 4.6 Transformer and its equivalent π model

Based on the original transformer's parameters, the equivalent line parameters can be found in (4.10)

$$\begin{aligned} G_{ij} &= \frac{G_T}{t}, G_{i0} = G_T \frac{1-t}{t^2}, G_{j0} = G_T \frac{t-1}{t} \\ B_{ij} &= \frac{B_T}{t}, B_{i0} = B_T \frac{1-t}{t^2}, B_{j0} = B_T \frac{t-1}{t} \end{aligned} \tag{4.10}$$

Hence, the line reactive power flow will be

$$Q_{ij} = -V_i^2 B_T \frac{1}{t^2} - V_i V_j \frac{1}{t}(G_T \sin\delta_{ij} - B_T \cos\delta_{ij}) \tag{4.11}$$

The total line reactive flow change can be expressed as:

$$\Delta Q_{ij} = \frac{\partial Q_{ij}}{\partial t}\Delta t + \frac{\partial Q_{ij}}{\partial V_i}\Delta V_i + \frac{\partial Q_{ij}}{\partial V_j}\Delta V_j \tag{4.12}$$

And, as to this bus, the variance of bus reactive power should be zero, so we have

$$\Delta Q_i = \sum_j \left[\frac{\partial Q_{ij}}{\partial t}\Delta t + \frac{\partial Q_{ij}}{\partial V_i}\Delta V_i + \frac{\partial Q_{ij}}{\partial V_j}\Delta V_j \right] = 0 \tag{4.13}$$

Notice that the first term is only shown for the LTC branch.

Comparing the equation (4.5), the only change is the branch parameters. That is, the new bus current should include the new branch parameters by considering the tap changes. Thus, the new expression should be:

$$\begin{aligned} &\sum_j \{[(V_i + \Delta V_i)\angle\delta_i - (V_j + \Delta V_j)\angle\delta_j](G_{ij} + jB_{ij})\} + (V_i + \Delta V_i)\angle\delta_i \sum_j (G_{ij0} + jB_{ij0}) \\ &+[(V_i + \Delta V_i)\angle\delta_i - (V_j + \Delta V_j)\angle\delta_j]\frac{1}{(t+\Delta t)}(G_T + jB_T) + (V_i + \Delta V_i)\angle\delta_i \frac{1-(t+\Delta t)}{(t+\Delta t)^2}(G_T + jB_T) \\ &+\left[\frac{-j(Q_s + \Delta Q_s)}{(V_i + \Delta V_i)\angle\delta_i}\right]^* + \left[\frac{P_i + jQ_i}{(V_i + \Delta V_i)\angle\delta_i}\right]^* = 0 \end{aligned} \tag{4.14}$$

Now, the three equations like those for shunt devices can be built:

$$-p_i\Delta t = \Delta V_i \sum_j^{n_j} a_{ij} + \Delta V_1 b_{i1} + \ldots + b_{in_j}\Delta V_{n_j} \tag{4.15}$$

$$-[\sum_j^{n_j}(h_{ij} + k_{ij}) + g_i] = \Delta V_i[\sum_j^{n_j}(c_{ij} + e_{ij}) + f_i] - \Delta V_1 d_{i1} - \Delta V_2 d_{i2} - \ldots - \Delta V_{n_j} d_{in_j} \tag{4.16}$$

$$-[\sum_{j}^{n_j}(\bar{h}_{ij}+\bar{k}_{ij})+\bar{g}_i]=\Delta V_i[\sum_{j}^{n_j}(\bar{c}_{ij}+\bar{e}_{ij})+\bar{f}_i]-\Delta V_1\bar{d}_{i1}-\Delta V_2\bar{d}_{i2}-\ldots-\Delta V_{n_j}\bar{d}_{in_j} \quad (4.17)$$

The symbols in (4.15), (4.16) and (4.17), which are the same in (4.7), (4.8) and (4.9), have the same definitions as those in shunt device parts with $\Delta Q_s = 0$ and only for the LTC branch in (4.16) and (4.17) the updated branch parameters have to be applied:

$$G_{ij}=\frac{G_T}{t+\Delta t}, B_{ij}=\frac{B_T}{t+\Delta t}, G_{i0}=G_T\frac{1-(t+\Delta t)}{(t+\Delta t)^2}, B_{i0}=B_T\frac{1-(t+\Delta t)}{(t+\Delta t)^2}$$

Additionally, for (4.15)

$$p_i=\frac{2V_i^2B_T}{t^3}+\frac{V_iV_j}{t}(G_T\sin\delta_{ij}-B_T\cos\delta_{ij}).$$

3. Computation Method

For fast and local voltage predicting, the designed computation method is utilized to quickly achieve the centered bus voltage and the voltages of the buses which connect to the centered bus directly. First, this computation method is based on the hypothesis described in [16][17]: one control device has only limited geographical influent. Namely, the attenuate factor σ will be introduced. For instances, in equation (4.7), (4.8) and (4.9), ΔV_j can be represented as:

$$\Delta V_j=\sigma_j\Delta V \quad \text{s.t.} \quad \sigma_j\in(-1,1) \quad (4.18)$$

Secondly, only the (4.7) for one shunt device or (4.15) for one LTC will be used to solve the incremental voltages with (4.18) in order to relax the too many constrains on one centered bus and its neighbors. However, the calculated σ and the updated bus voltages have to satisfy the optimal objectives coming from equations (4.8) and (4.9) for one shunt device simultaneously or equations (4.16) and (4.17) for one LTC. The detailed method is formulated as follows:

$$\Delta V_i = \frac{\Delta}{\sum_j^{n_j} a_{ij} + \sigma_1 b_{i1} + \ldots + \sigma_{n_j} b_{in_j}}$$

s.t.

$$\min_{\sigma} \left\| f(\sigma) \right\|_2^2$$

as

$$f(\sigma) = \begin{bmatrix} \dfrac{[\sum_j^{n_j}(c_{ij}+e_{ij})+f_i]+(\sigma_1 d_{i1}-\sigma_2 d_{i2}-\ldots-\sigma_{n_j} d_{in_j})}{\sum_j^{n_j} a_{ij}+\sigma_1 b_{i1}+\ldots+\sigma_{n_j} b_{in_j}}\Delta+[\sum_j^{n_j}(h_{ij}+k_{ij})+g_i] \\ \dfrac{[\sum_{j=1}^{n_j}(\bar{c}_{ij}+\bar{e}_{ij})+\bar{f}_i]+(\sigma_1 \bar{d}_{i1}-\sigma_2 \bar{d}_{i2}-\ldots-\sigma_{n_j} \bar{d}_{in_j})}{\sum_j^{n_j} a_{ij}+\sigma_1 b_{i1}+\ldots+\sigma_{n_j} b_{in_j}}\Delta+[\sum_j^{n_j}(\bar{h}_{ij}+\bar{k}_{ij})+\bar{g}_i] \end{bmatrix} \quad (4.19)$$

$$\Delta = \Delta Q_i \; or - p\Delta t,$$

$$-1 < \sigma_i < 1$$

Implementing this computation method practically should consider two modes:

mode 1: if the LVP is for one shunt device, all attenuate factors are equal with the range [0,1] .

mode 2: if the LVP for one LTC, all attenuate factors except the one for the LTC branch are equal with the range [0,1] and the attenuate factor for LTC branch is with the range [-1,0].

mode 3: if the non-centered bus is PV bus, in the calculation process, it will be treated as PQ bus but the final incremental voltage change will be reset to zero.

4. Examples

Suppose that there are 10 MVAR capacitor switched in at Bus 9 of 9-bus system. The results from LVP and Power Flow are shown in Table 4.2.

Bus	V_0	$V_1(\sigma)$ from LVP	V_1 from PF	Error
Bus 9	0.9576	0.9668	0.9664	0.04%
Bus 8	0.9962	0.9981(0.3151)	0.9984	0.03%
Bus 4	0.9870	0.9898(0.3151)	0.9903	0.05%

Table 4.2 Results from LVP and PF for 10 Mvar capacitor on 9-bus system

The maximum estimation error is less than 0.1% so that this computation method has good performance for the shunt device.

For the tap change of one LTC, we use 30-bus test system. There is a LTC between Bus 6 and Bus 9 with tap ratio 0.978 in the base case. And if the tap ratio is decreased by 0.01, Table 4.3 shows the results from LVP and Power Flow.

Again, the maximum error of the estimation voltage by LVP after tap changing is so small that all the estimations are acceptable and accurate enough to prepare all the conditions which can be employed to decide the control actions.

Bus	V_0	$V_1(\sigma)$ from LVP	V_1 from PF	Error
Bus 9	1.0525	1.0479	1.0488	0.086%
Bus 6	1.0134	1.0139(-0.1)	1.014	0.001%
Bus 11	1.082	1.082(0) : PV bus	1.082	0.00%
Bus 10	1.0467	1.0444(0.5)	1.0444	0.00%

Table 4.3 Results from LVP and PF for tap changes on 30-bus system

4.2.3 Summary

In the entire Advance Voltage Controller scheme, the Local Voltage Predictor should present the voltages of the local buses quickly and accurately. By the above test cases, the designed LVP works as proposed. LVP has the main-backup structure. Model-free LVP takes full advance of Synchrophasors so that its calculation is super fast and simple. On the other hand, Model-Based LVP will do more calculation with network parameters and SE solution. And some tuning stuff will be done before usage. However, this process is fast enough as well since we do not use the entire network and only local control system is taken account into.

4.3 Optimized Control Decision

4.3.1 Formulation Design

Among the candidate control devices in the local system and after the controller already knows their effects of control actions, the next problem is to find the right one which can satisfy some requirements like minimizing the switching cost besides mitigating the bus voltage issues.

Obviously, there is not such a rule which restricts this optimization. The vision is still open. In this dissertation, several practical rules and preference used by system operators

are considered. In detail, we have to put the effect of control action into the formulation first since this is the main goal of the controller. But, the control strategy is to mitigate the bus voltage violation or increase the voltage stability level so that LVP can provide the desired amount for each control action. That is, if one calculation from LVP is not able to solve the current voltage issues, LVP will be triggered again and again until two facts have been met: i) all voltage violations vanish or the voltage stability level is increased; ii) all devices are exhausted. Based on the designs, only model-based LVP will experience this process while model-free LVP will give the results directly. However, we have to use the virtual reactive power injection changes caused by tap changing at two endings of that LTC to calculate the desired tap.

$$\Delta t = \frac{\Delta Q_{Ti}}{-\frac{\partial Q_{ij}}{\partial t}} = -\frac{\Delta Q_i}{\frac{V_i^2}{t^3} B_T - \frac{Q_{ij}}{t}} \tag{4.20}$$

Or,

$$\Delta t = \frac{\Delta Q_{Ti}}{-\frac{\partial Q_{ij}}{\partial t}} = -\frac{\Delta Q_i}{\frac{V_j^2}{t} B_T - \frac{Q_{ji}}{t}} \tag{4.21}$$

Secondly, the device switching cost will be counted as well because some devices can't switching frequently, which should have higher costs. And for ensuring the maximum number of the available control devices, switching out device should be given

lower cost than switching in device. Like the system operators' practice, LTCs may have higher priority than the shunt reactive compensation devices so that LTCs will be more "expensive" when they are deployed.

With the above considerations, this optimization problem is formulated as follows[16]:

$$\begin{aligned}
&\min: \sum_{i=1}^{N_{device}} \left\{ c_i \left[t_i |k_i| \left| T_i^{desired} - T_i^{current} \right| + q_i |k_i| \left| Q_i^{desired} - Q_i^{current} \right| \right] \right\} \\
&s.t.: \ V_{j\min} \le V_j \le V_{j\max}; j = 1,2,...,N_{bus} \\
&\quad T_{i\min} \le T_i \le T_{i\max}; \\
&\quad Q_{si\min} \le Q_i \le Q_{si\max} \\
&k_i \in \{-1,0,1\}
\end{aligned} \tag{4.22}$$

In (4.22), t_i and q_i are the device effect factors for LTCs and shunt reactive power compensation devices respectively. For certain bus i, t_i and q_i cannot be effective in the same time. That is, when one shunt device has been used, t_i will be zero and vice versa. Correspondingly, $T_i^{desired}$ and $Q_i^{desired}$ are the desired taps and compensation resulting from LVP while $T_i^{current}$ and $Q_i^{current}$ are the current values. The third term is mainly for switching costs. In that, c_i is the device cost. k_i represents the device switching status. "-1" means switching out, "0" is for no switching and "1" for switching in.

The objective of this optimization formulation is to minimize the total control action cost meanwhile all the bus voltages should be within their user-defined limits and all control device regulations be in their physical limits.

The candidate control actions with the desired taps or the compensation amount come from LVP. Simply, if only one device can be switched in one time, and then this formulation will compare all control action costs by going through all actions. But, if some desired control action exceeds its own physical limit, that limit will be used to replace that desired control action with much bigger effective factor than normal. Since one local control area should not have many buses and numerical control devices, this "greedy" calculation process would not be time-consuming but can guarantee the solution is locally optimized. More, in certain linear operation area, superposition law is still suitable so that multi-switching can be considered by this "greedy" method too. Essentially, there is no big difference. But the practical way is to get the "best" devices with minimum costs step by step because only one device is not sufficient to solve the most voltage issue completely. In each step, the correspondingly "best" device is chosen and the voltage issue is released a little. And then, the next "best" one will base on this new condition. Apparently, this requires the iteration among LVP and optimization block, however, the calculation processes for themselves are not changed.

4.3.2 Example

In the following section, the preliminary tests in IEEE 30-bus system will be given in order to demonstrate the process of making optimal control decision.

The rules are constructed first: the cost for switching out a shunt device is set to zero, the cost for switching in a shunt device is set 10.0, the cost for LTC tap changing is set to 20.0*n (n is the number of changes). After some scenarios, the control devices are used to resume the bus voltages within 2% range around the base case voltage profile. Table 4.4 shows the control devices in the system.

Device Type	Bus/Transformer	Range	Status
Shunt	Bus 5	19.0	ON
	Bus 14	10.0	OFF
	Bus 15	10.0	OFF
	Bus 16	10.0	OFF
	Bus 17	10.0	OFF
	Bus 24	4.3	ON
LTC	Bus 6 ->| Bus 9	0.938 ~ 1.018	0.978
	Bus 6 ->| Bus 10	0.929 ~ 1.009	0.969
	Bus 4 ->| Bus 12	0.892 ~ 0.972	0.932
	Bus 28 ->| Bus 27	0.928 ~ 1.008	0.978

Table 4.4 Control devices in 30-bus system

Assume one scenario is set to increase the load at Bus 16 by 50 MW and 10MVAR. Table 4.5 shows the biggest five voltage deviations comparing the base case.

Bus Number	V_0	V_L	ΔV	V_{des}	ΔV_{des}
16	0.9866	0.9376	-0.049	0.9669	0.0293
17	0.9817	0.9633	-0.0184	0.9621	-0.0012
4	0.9669	0.9564	-0.0105	0.9476	-0.0088
8	0.9488	0.9385	-0.0103	0.9298	-0.0087
6	0.9618	0.9514	-0.0104	0.9426	-0.0088

Table 4.5 Bus voltages the biggest five deviations after load increasing

In the first step, Bus 16 needs to be controlled in order to make its voltage back into the required range [0.9669, 1.008]. Table 4.6 shows the desired control actions by the desired voltage change and the corresponding switching cost. Notice that the LTCs between 6 and 9, between 6 and 10 and between 27 and 28 are far away from Bus 16 relatively, we do not show the information about them. And switching off a capacitor will not be helpful, the capacitors in Bus 5 and Bus 24 will be ignored as well.

Control Device	Available Capacity	Desired Capacity	Cost
Cap at Bus 16	0.10	0.1813	0.813
Cap at Bus 17	0.10	0.4334	3.334
Cap at Bus 12	0.10	0.6316	5.136
Cap at Bus 14	0.10	0.7936	6.636
LTC Bus 12 ->| Bus 4	0.892 ~ 0.972	0.892	80

Table 4.6 Control options in the first step

Clearly, the capacitor in Bus 16 is the best choice in the first step although the bus voltage violations are still existing. In the same way, the ALVC will pick up the control device to eliminate or mitigate the voltage violations eventually. Table 4.7 displays the whole control actions.

Step #	V_{worst} (Before Control)	ΔV_{des}	Control Device	Action	V_{worst} (after Control)
1	Bus 16 0.9376	0.0293	Bus 16 10 Mvar	ON	Bus 16 0.9537
2	Bus 16 0.9537	0.0132	Bus 17 10 Mvar	ON	Bus 16 0.9604
3	Bus 16 0.9604	0.0065	Bus 12 10 Mvar	ON	Bus 16 0.9650
4	Bus 16 0.9650	0.0019	LTC Bus 12 ->| Bus 4	0.932 -> 0.922	Bus 16 0.9666
5	Bus 16 0.9666	0.0003	Bus 14 10 Mvar	ON	No Violation

Table 4.7 Control actions on 30-bus system when load increasing at Bus 16

In this test, we have given sufficient control devices which include small capacity of shunt capacitors. If the given control devices change, the control action will differ from those in Table 4.7. For example, if there is big capacity in Bus 17, saying 40 Mvar, based on the calculation in Table 4.6, the first control device should be that in Bus 17, which has the switching cost 0.334 less than the 0.813 for the capacitor at Bus 16.

4.4 Summary

The Advanced Local Voltage Controller has been well-defined in this chapter. Its design is considerable and comprehensive. For one thing, this controller can apply Synchrophasors as inputs so that the model-free control process can be possible with the help of the proposed Mode-free Local Voltage Predictor. For another, one redundant control process, which is so-called model-based, is developed to parallel that model-free one as the back-up. The difference is about how to predict the voltage changes after control actions. In this situation, SCADA and SE are the data sources. Actually, these two processes can work independently from each other. When one data source is not reliable or not available, the other one can accomplish the control task without any doubt. In normal conditions, the model-free control process is treated as the main one because of its simple and direct calculation and less requirement for the parameters.

No matter which control process is deployed, the final control action(s) must be optimized choice because the influences from control actions and the device switching costs are taken account into the design simultaneously.

Chapter 5

Conclusions and Future Work

5.1 Conclusions

Motivated by the wide applications of Synchrophasors and installations of PMUs in the world, methods to take advantage of this faster and more accurate measurement data sources have been developed to assess the voltage stability and control the voltages has been in our considerations. This dissertation has presented a full series of designs from real-time voltage stability monitoring to real-time voltage control by using Synchrophasors.

The theoretical foundation of the feasibility of the real-time voltage stability monitoring is indicated first because the monitoring process will utilize two new defined quantities: the line sensitivity and the global VSA index. By the analysis in static power flow and comparing with many classical voltage stability analysis methods, the consistency among them has been demonstrated. Certainly, a number of test cases have been shown for supporting.

Actually, the line sensitivity is the basis and serve as the methodology to apply Synchrophasors to assess voltage stability in real time. It is believed that Synchrophasors have contained sufficient information. Hence, two methodologies have been developed and explained in detail to show how they estimate the line sensitivities fast and accurately. many tests based on Synchrophasors coming from simulated test systems and actual measurements from real systems were used to test and to illustrate the algorithms.

The Advanced Local Voltage Controller is another novel improvement by importing Synchrophasors as the data source besides SCADA/SE. Two Local Voltage Predictors are proposed to estimate voltage changes after certain control action because this controller focuses on the control in substation level and then the full power flow is not proper any more. One of them has model-free structure since it only deals with Synchrophasors while the other demands the measurement and results from SCADA/SE. They have their own prediction procedures but the predicted results should be the same or not be different so much. Besides mitigating the voltage violations and releasing the potential voltage stability troubles, this controller will provide the “best” choices with minimum control action costs.

5.2 Future Work

As the research goes further, there must be some important works which need to be done to polish or even improve our designs.

First all, the tests on the Advanced Local Voltage Control by using real power system data should be pursued. This process may include the testing about two LVPs and the testing about optimization block respectively.

Second, task should be the implementation of a prototype of whole monitoring and control system by using Synchrophasors and SCADA/SE.

Some other work such as the visualization of the results of real time voltage monitoring can make them more convenient to be observed. More complex optimization formulation can make the control actions meet more demands from the real power systems.

Bibliography

[1] www.truststc.org/scada/papers/paper34.pdf

[2] http://www05.abb.com/global/scot/scot296.nsf/veritydisplay/2d4253f3c1bff3c0c12572430075 caa7/$file/ed itorial_2001_04_en_pmus_-_a_new_approach_to_power_network_monitoring.pdf

[3] Phadke A.G. "Synchronized phasor measurements-a historical overview", IEEE/PED Transmission and Distribution Conference and Exhibition 2002: Asia Pacific, vol. 1, pp. 476 - 479.

[4] http://openpdc.codeplex.com/

[5] P. Kundur, *Power System Stability and Control*. McGraw-Hill, inc., New York, 1994.

[6] Donolo, M.; Venkatasubramanian, M.; Guzman, A.; de Villiers, F., " Monitoring and Mitigating the Voltage Collapse Problem in the Natal Network", *Power System Conference and Exposition 2009*, pp. 1-5, 2009.

[7] Yanfeng Gong, Schulz N., Guzman A., "Synchrophasor-Based Real-Time Voltage Stability Index", *Power Systems Conference and Exposition 2006*, pp. 1029-1036, 2006.

[8] N. Amjady, "Voltage Security Evaluation by a New Framework based on the Load Domain Margin and Continuation Method", Power Engineering Society General Meeting, 2005. IEEE, vol. 3, pp. 2914-2920, June. 2005.

[9] Ruisheng Diao, Kai Sun, Vittal V., O'Keefe R.J., Richardson M.R., Bhatt N., Stradford D., Sarawgi S.K., "Decision Tree-Based Online Voltage Security Assessment Using PMU Measurements", *IEEE Transactions on Power Systems*, Volume 24, Issue 2, pp. 832-839, 2009.

[10] M. L. Liu, B. Z. Zhang, Y. M. Han, H. B. Sun and W. H, Wu, "PMU Based Voltage Stability Analysis for Transmission Corridors". Apr. 2008, Electric Utility Deregulation and Restructuring and Power Technologies, Third International Conference. pp. 1815-1820.

[11] M. Parniani, J. H. Chow, L. Vanfretti, B. Bhargava and A. Salazarm, "Voltage Stability Analysis of a Multiple-Infeed Load Center Using Phasor Measurement Data", Oct. 2006, Power Systems Conference and Exposition, 2006. PSCE '06. 2006 IEEE PES. pp. 1299-1305.

[12] Verbic G., Gubina F., "Protection Against Voltage Collapse Based on Local phasors", *Power Tech Proceedings 2001*, Volume 4, 2001.

[13] Raczkowski B.C., Sauer P.W., "Identification of Critical Cutsets for Static Collapse Analysis", *Bulk Power System Dynamic and Controll – VII. Revitalizing Operational Reliability, 2007 iREP Symposium*, pp. 1-8, 2007.

[14] S. Grijalva and P.W. Sauer, "A necessary condition for power flow Jacobian singularity based on branch complex flows," *IEEE Transactions on Circuits and Systems I,* vol. 52, issue 7, pp.1406-1413, July 2005.

[15] Ajjarapu V., Christy C., "The Continuation Power Flow: A Tool for Steady State Voltage Stability

Analysis", *Power Industry Computer Application Conference, 1991. Conference Proceedings*, pp 304-311, 1991.

[16] Y. Chen, *Development of Automatic Slow Voltage Control for Large Power Systems*, Ph.D. dissertation, School of Electrical Engineering and Computer Science, Washington State University, Pullman, WA, August 2001.

[17] J. Su, *A Heuristic Slow Voltage Control Scheme for Large Power Systems*, Ph.D. dissertation, School of Electrical Engineering and Computer Science, Washington State University, Pullman, WA, August 2006.

[18] X.Yue and V. Venkatasubramanian, "Complementary Limit Induced Bifurcation Theorem and Analysis of Q limits in Power-Flow Studies", Bulk Power System Dynamics and Control-VII. Revitalizing Operational Reliability, 2007 iREP Symposium, pp. 1-8, 19-24 Aug. 2007.

[19] http://www.pserc.cornell.edu/matpower/

[20] Guoping Liu, J. Quintero, and Vaithianathan "Mani" Venkatasubramanian, "Oscillation Monitoring System Based on Wide Area Synchrophasors in Power Systems", Aug. 2007. Bulk Power System Dynamics and Control - VII. Revitalizing Operational Reliability, 2007 iREP Symposium, pp. 1 – 13.

[21] B. Gao, G.K. Morison, L. Wang, and P. Kundur, "Voltage stability evaluation using modalanalysis", *IEEE Trans. on Power System,* vol. 7, no. 4, pp. 1529-1542, Nov. 1992.

[22] K. Morison, L. Wang and P. Kundur, “Power System Security Assessment”, *IEEE Power & Energy Magazine,* pp. 30-39 September/October, 2004.

[23] Y. Yu, J. Sun, G. Zheng, Q. Lou, Y. Min, and Y. Song, “ On-line Voltage Secruity Assessment of the Beijing Power System”, Electric Utility Deregulation and Restructuring and Power Technologies, 2008. DRPT 2008. Third International Conference *on 6-9,* pp.684-688, April. 2008.

[24] K.C. Hui, M. J. Short, “A neural networks approach to voltage security monitoring and control”, Neural Networks to Power Systems, 1991., Proceedings of the First International Forum on Applications of

23-26, pp. 89-93, July 1991.

[25] M. Pandit, L. Srivastav, and J. Sharma, “Fast voltage contingency selection using fuzzy parallel self-organising hierarchical neural network”, *IEEE Trans. on Power System,* vol. 18, no. 2, pp. 162-172, 1994.

[26] H. Liu, A. Bose, and V. Venkatasubramanian, “ A Fast Voltage Security Assessment Method Using Adaptive Bounding”, *IEEE Trans on Power System,* vol. 15, no. 3, August. 2000.

[27] G. Huang, and T. Zhu, “Voltage Security Assessments Using the Arnoldi Algorithm”, vol. 2, pp. 635-640, July. 1999.

[28] N.P. Patidar and J. Sharma, "Case-Based Reasoning Approach to Voltage Security Assessment of Power System", Industrial Technology, 2006. ICIT 2006. IEEE International Conference on *15-17,* pp. 2768-2772, Dec. 2006.

[29] N.C. Chang, J. F. Su, Z. B. Du, L. B. Shi, H. F. Zhou, Peter T. C. Tam, Y. X. Ni, Felix F. Wu, "Developing a Voltage-Stability-Constrained Security Assessment System", *IEEE/PES Transmission and Distribution Conference & Exhibition: Asia and Pacific,* pp. 1-5, 2005.

[30] I.Dobson and H.D.Chiang, "Towards a theory of voltage collapse in electric power systems", *Systems and Control letters*, vol. 13, no. 3, pp. 253-262, 1989.

[31] C. W. Taylor, Power System Voltage Stability, McGraw-Hill, inc., New York, 1992.

[32] E. O. Schweitzer, III and David E. Whitehead, "Real-World Synchrophasor Solutions", Oct. 2008, *35th Annual Western Protective Relay Conference*, Section IX.

[33] M. L. Liu, B. Z. Zhang, Y. M. Han, H. B. Sun and W. H, Wu, "PMU Based Voltage Stability Analysis for Transmission Corridors". Apr. 2008, Electric Utility Deregulation and Restructuring and Power Technologies, Third International Conference. pp. 1815-1820.

[34] J.P. Paul, J.T. Leost, J.M. Tesseron, "Survey of the Secondary Voltage Control in France: Present Realization and Investigations," IEEE Transactions on Power Systems, vol. PWRS-2, no.2, pp. 505-511, 1987.

[35] T.V.Cutsem, "Voltage Instability: Phenomena, Countermeasures, and Analysis Methods", *Proceedings of IEEE,* Vol. 88, No. 2, pp. 208-227, February 2000.

APPENDIX

The one-line diagrams of the test systems in this dissertation are shown as follows. The corresponding data can be found in the MATPOWER package [].

IEEE 9 Bus Test System

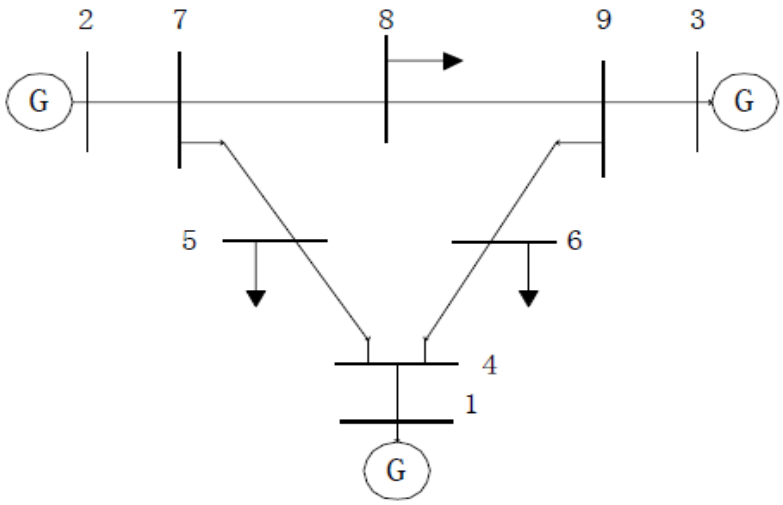

Figure A.1 One-line diagram of IEEE 9 bus test system

IEEE 30 Bus Test System

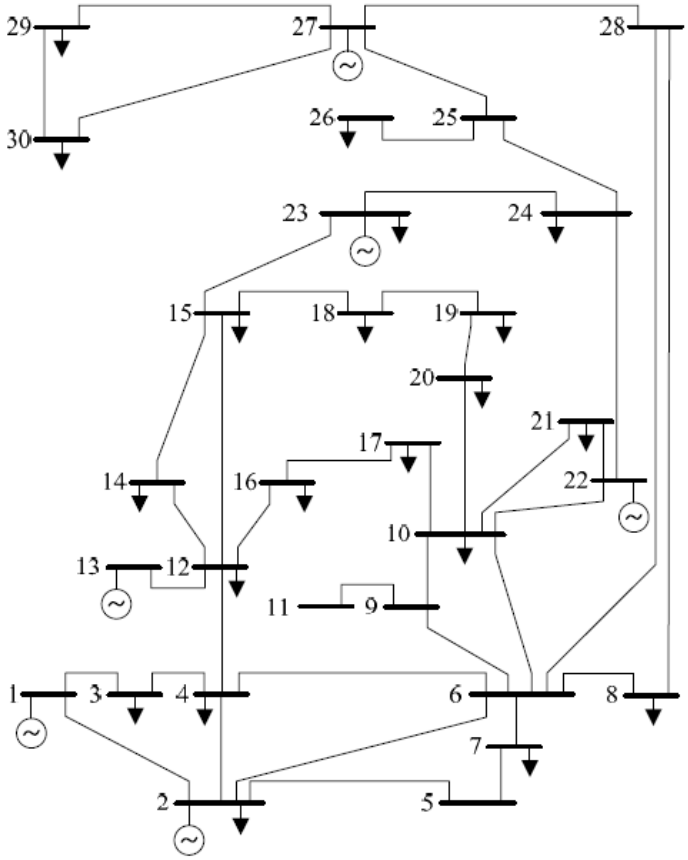

Figure A.2 One-line diagram of IEEE 30 bus test system

New England 39 Bus Test System

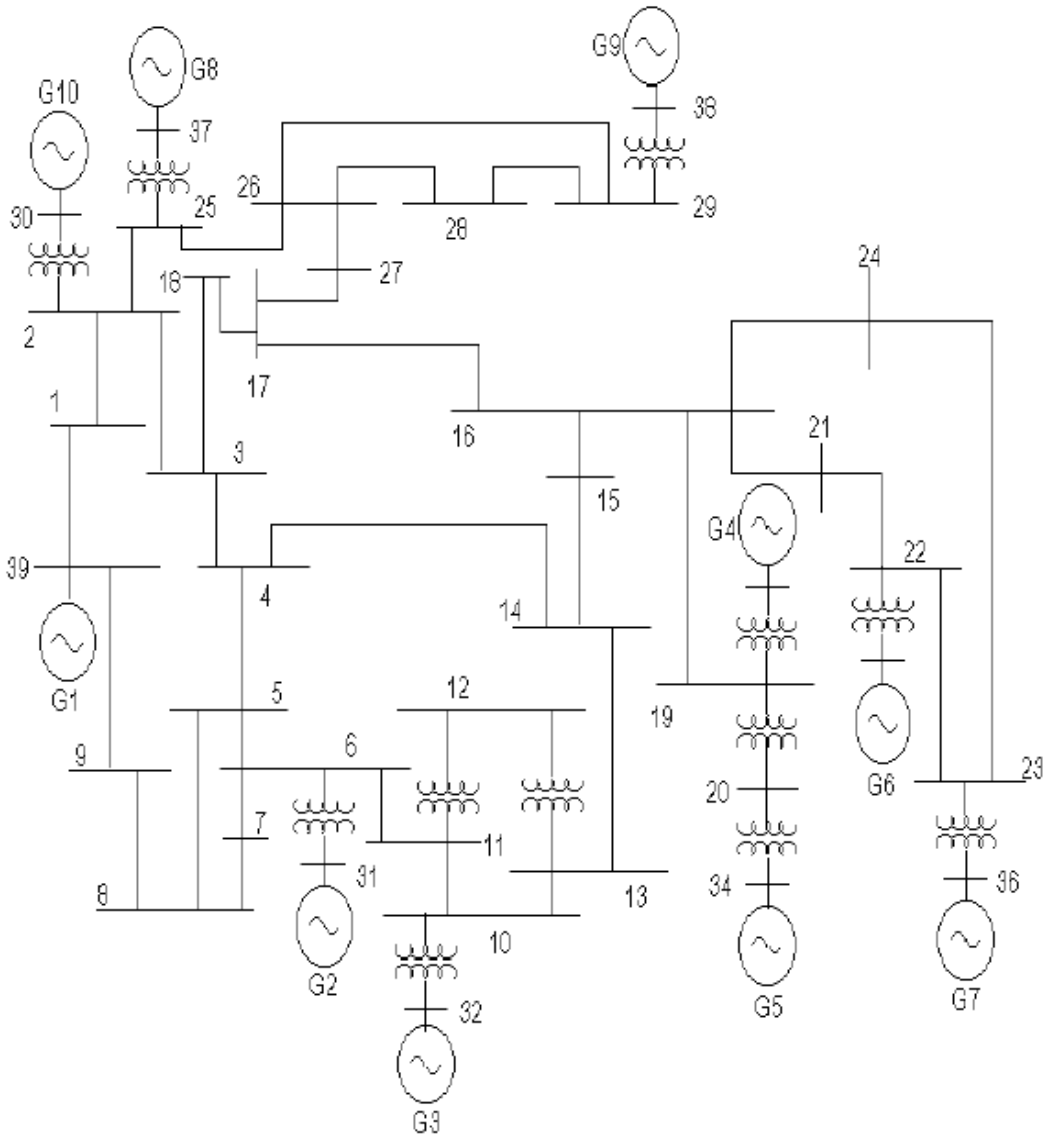

Figure A.3 One-line diagram of New England 39 bus test system

IEEE 300 Bus Test System

This one-line diagram of IEEE 300-bus system is just for illustration. The bus numbers used in this dissertation are different with those in the following graphs.

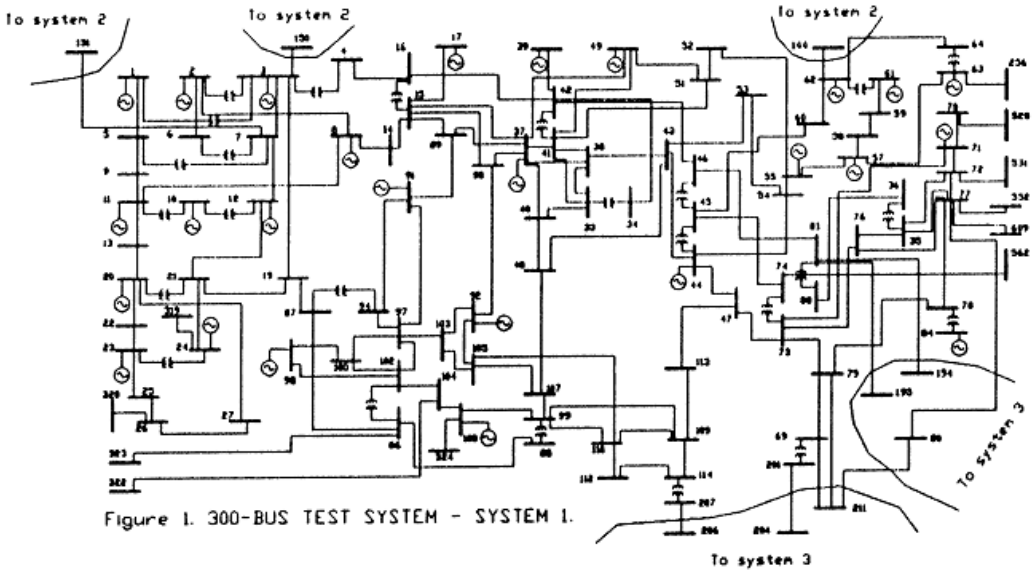

Figure A.4 One-line diagram of IEEE 300 bus test system-system 1

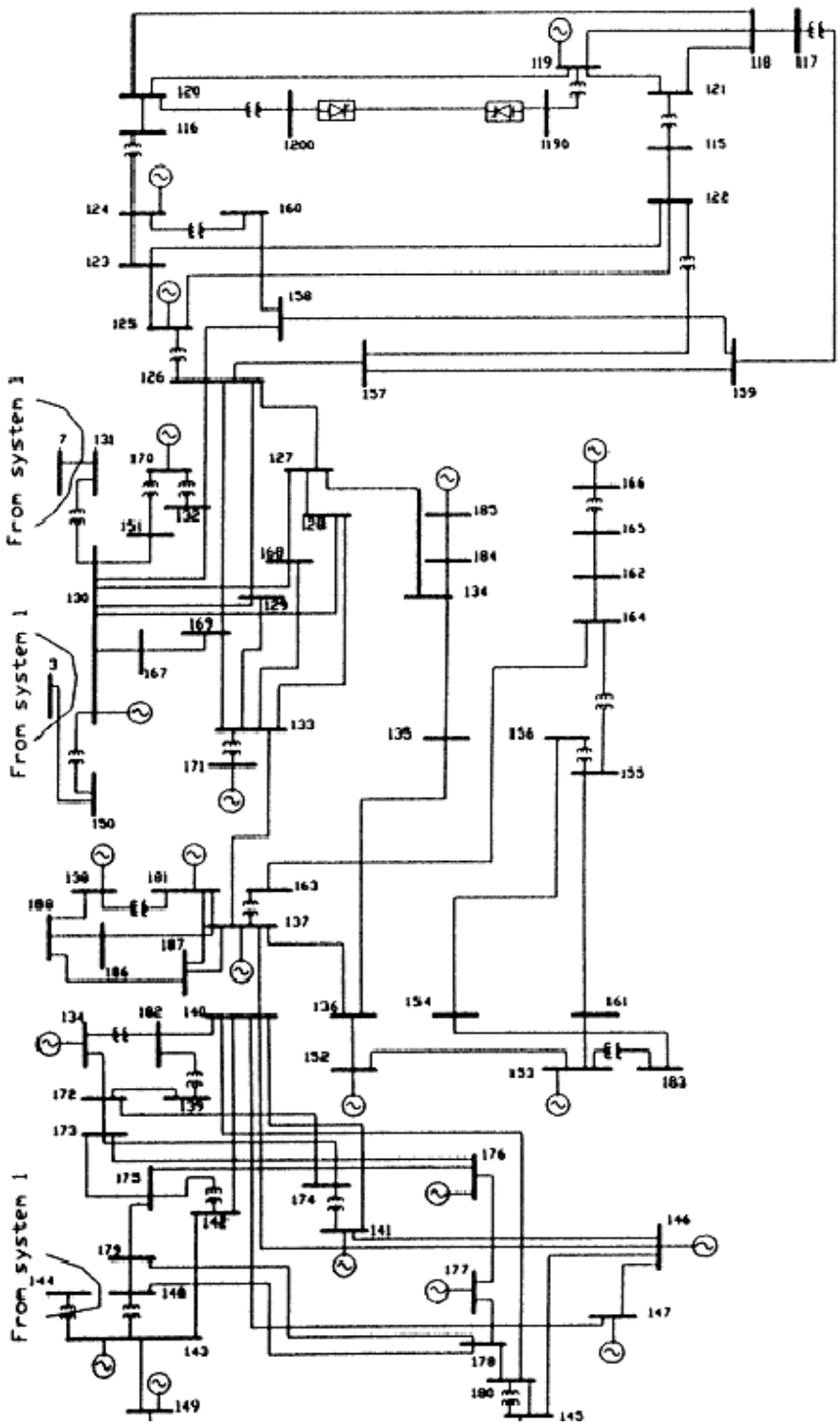

Figure A.5 One-line diagram of IEEE 300 bus test system-system 2

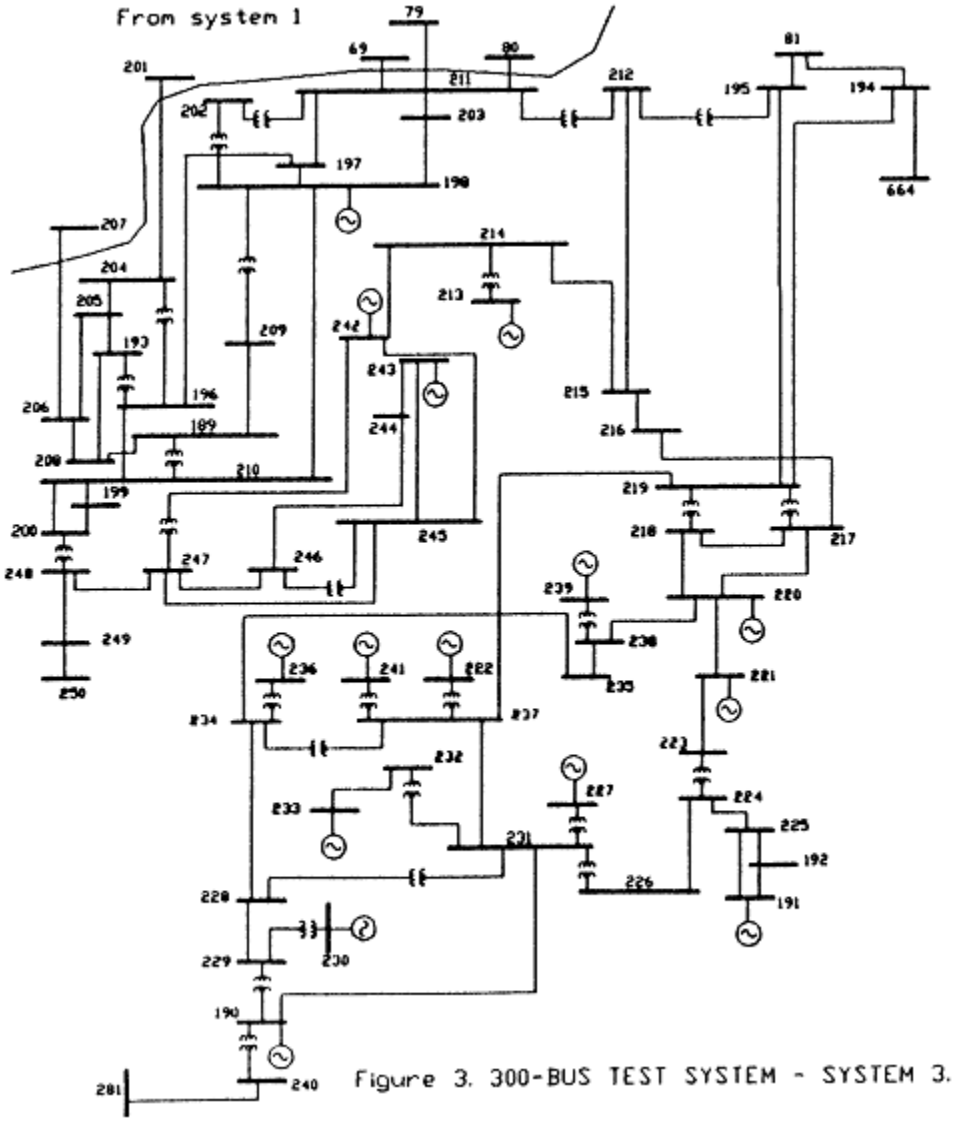

Figure A.6 One-line diagram of IEEE 300 bus test system-system 3